Chapter 4

Modified Quadratic Gain Bidirectional DC-DC Converter

4.1 Introduction

Chapter 3 Quadratic gain bidirectional converter (QGBC) has been modified and designed with a reduced number of components. The modified QGBC has only four power switches and the voltage conversion gain is the same as the converter in previous chapter 3. The modified QGBC has eliminated two power diodes. Therefore the converter size, losses are reduced and the efficiency of the converter is increased. In this chapter, the modified QGBC is connected to a load as shown in Figure 4.1. The load consist of a VSI fed Permanent magnet brushless DC (PMBLDC) motor and it is coupled with the pulley-belt arrangement. The proposed converter has the following advantages: high voltage gain at a low duty cycle, fewer power switches, a simple construction, and easy control. The converter is operated in continuous inductor current mode (CICM). For Regenerative braking (RB) of PMBLDC motor, the self-inductance of the motor is exploited to step up the back-Electromotive force (EMF) of the motor to extract the energy even at low rotor speed.

A brief outline of the chapter is as follows:

- Section 4.2 describes the converter's operation in step-up or motoring mode and step-down or regenerative braking mode.
- Section 4.3 gives the details of converter design and stability analysis.

- Section 4.4 described simulation and experimental results.
- The conclusion of the work is given in section 4.5

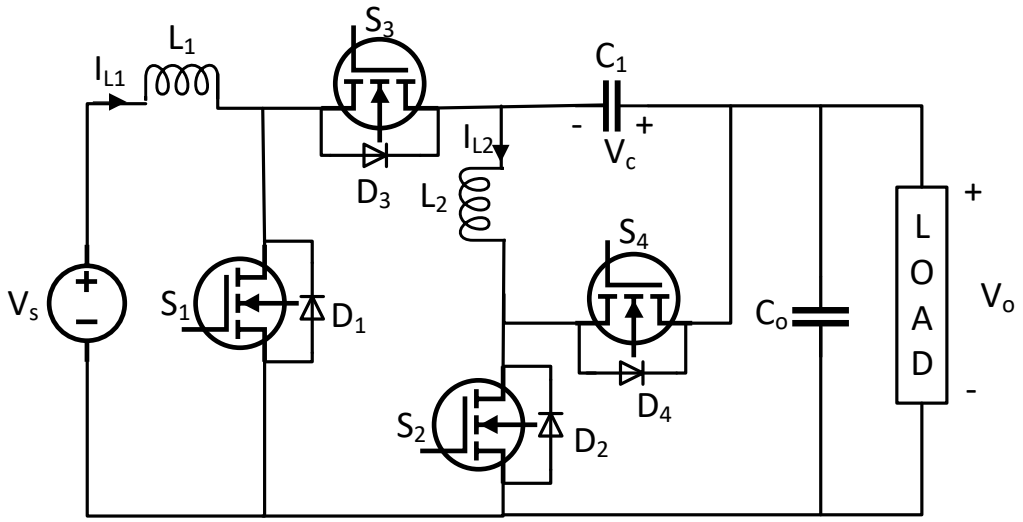

Figure 4.1: The topology of modified quadratic gain bidirectional DC-DC Converter.

4.2 Operation of the converter

The presented modified QGBC with battery and load is illustrated in Figure 4.1. Where V_s input voltage, V_c voltage across capacitor C_1, V_o output voltage, I_{L1} indcutor current of L_1, and I_{L2} inductor current of L_2. In the proposed converter consist of four power switches S_1, S_2, S_3, and S_4 with antiparallel diode. The converter's operation in the step-up the switches S_1, S_2 are controlled and converter's operation in the step-down the switches S_3, S_4 are controlled. The load on the converter consist of VSI fed PMBLDC motor with a belt-drum arrangement in the converter's step-up operation.

4.2.1 Step-up or Motoring Mode Operation

The converter's step-up operation are describe in two different stage. In step-up mode, transfer of energy from battery to load through controlled switches S_1 and S_2. The capacitor C_o supply enegry to load, inductor L_2 current increase,and capacitor C_1 charges. The working waveform of converter's operation in step-up mode is describe in Figure 4.4.

Stage- I (t_o, t_1): In this stage the S_1 and S_2 switches are ON and S_3 and S_4 switches

are OFF for the time interval of DT_s. The inductor L_1 current is increasing and energy is transfer to inductor from battery. The current conduction path of the converter in this stage is shown in Figure 4.2.

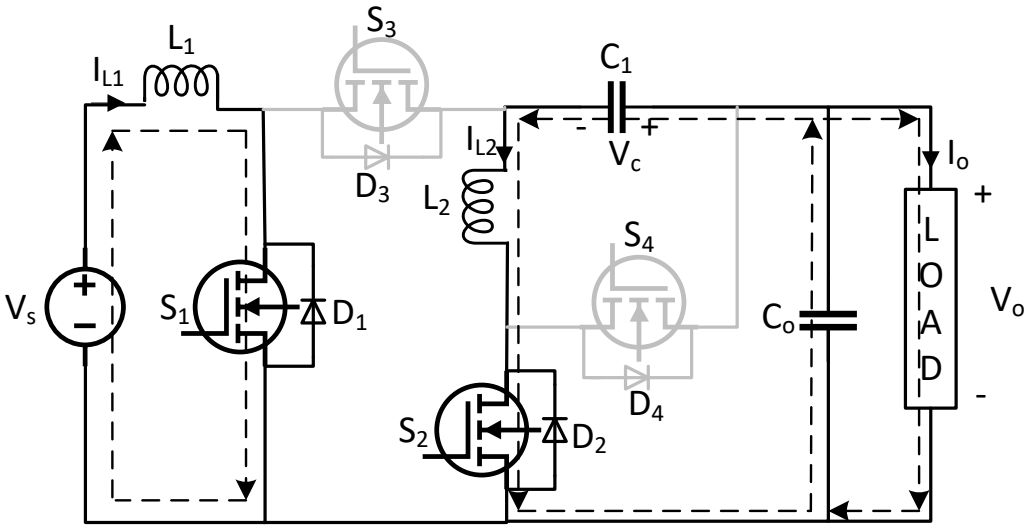

Figure 4.2: Current flowing path during step-up mode operation of converter in stage-I.

Stage-II (t_1, t_2): In this stage all the switches S_1, S_2, S_3, and S_4 are OFF for time interval (1-D)T_s. The stored enegry in indcutor L_1 and inductor L_2 is transfer to load. During this interval both inductors current decreases. The current conduction path of the converter in this stage is shown in Figure 4.3. Application of Volt-sec balance principle

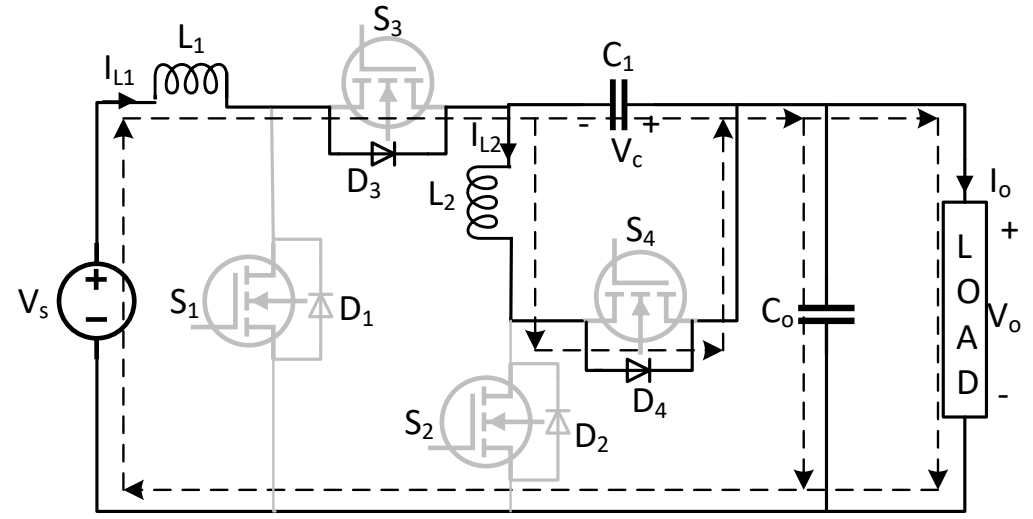

Figure 4.3: Current flowing path during step-up mode operation of converter in stage-II.

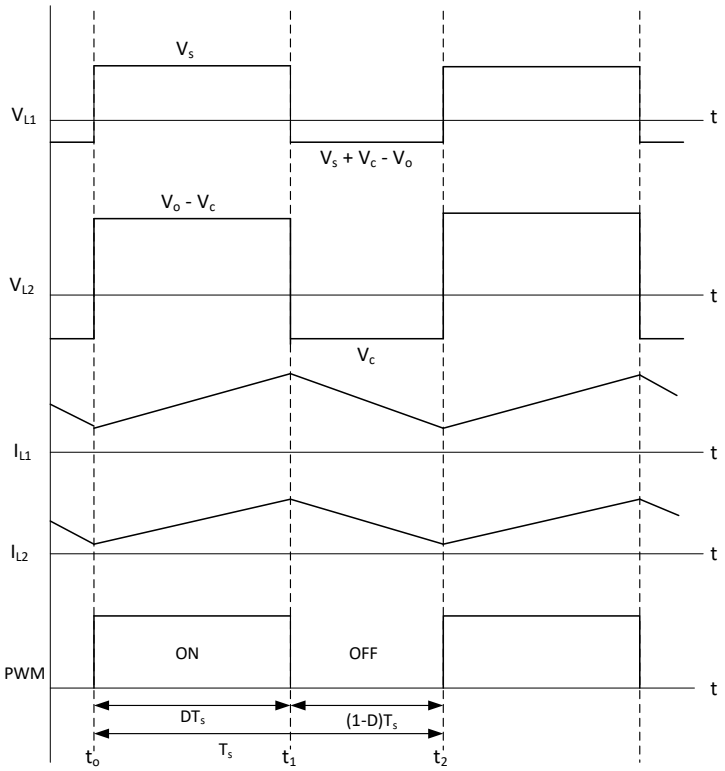

Figure 4.4: The working waveform of converter's operation in step-up mode.

on indcutor L_1 and L_2 the following equation obtained:

$$DV_s + (1 - D)(V_s + V_c - V_o) = 0 \tag{4.1}$$

$$D(V_o - V_c) + (1 - D)V_c = 0 \tag{4.2}$$

By eliminating V_c from eq. (4.1) and (4.2), the output voltage during step-up operation is obtained in eq. (4.3) quadratic in nature.

$$V_o = \frac{V_s}{(1 - D)^2} \tag{4.3}$$

The Voltage across capacitor C_1 is obtained as

$$V_c = DV_o = \frac{DV_s}{(1 - D)^2} \tag{4.4}$$

4.2.2 Step-down or Regenerative Braking Mode Operation

The step-down mode operation of converter are describe in two different stage. In RB operation of converter, the energy is transfer from load to battery by controlling switches S_3 and S_4. The working waveform of converter during regenerative braking is described

in Figure 4.7.

Stage- I (t_o, t_1): In this stage the switches S_3 and S_4 are ON and switches S_1 and S_2 are OFF during the time interval DT_s. During this interval both inductor's current increases and energy transferred from higher voltage to lower voltage. The current flowing path the converter in this stage is shown in Figure 4.5.

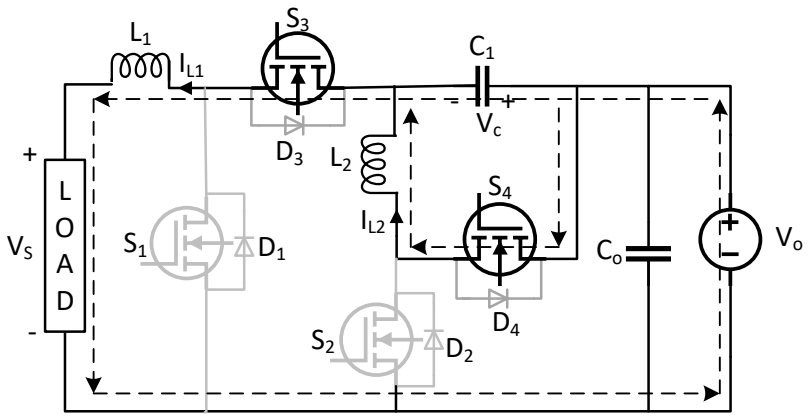

Figure 4.5: Current flowing path during step-down operation of the converter in stage-I.

Stage- II (t_1, t_2): In this stage all switches S_1, S_2, S_3 and S_4 are OFF during the interval (1-D)T_s. During this interval the stored energy in inductor L_1 is transfer to load and the energy stored in inductor L_2 is transfer to capacitor C_1. The current flowing path of operation in this stage is shown in Figure 4.6.

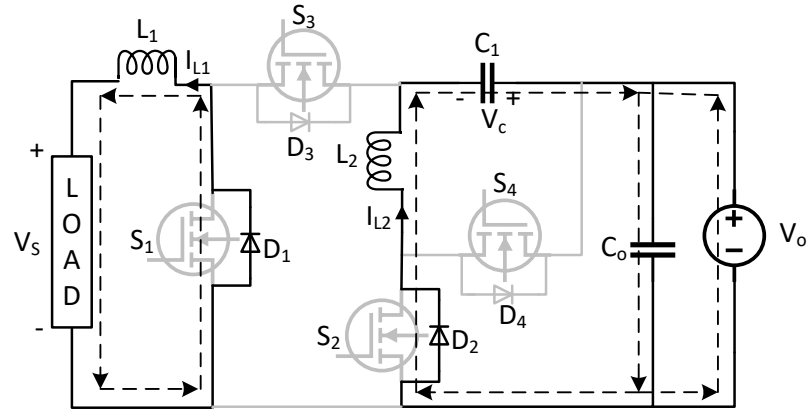

Figure 4.6: Current flowing path during step-down operation of the converter in stage-II.

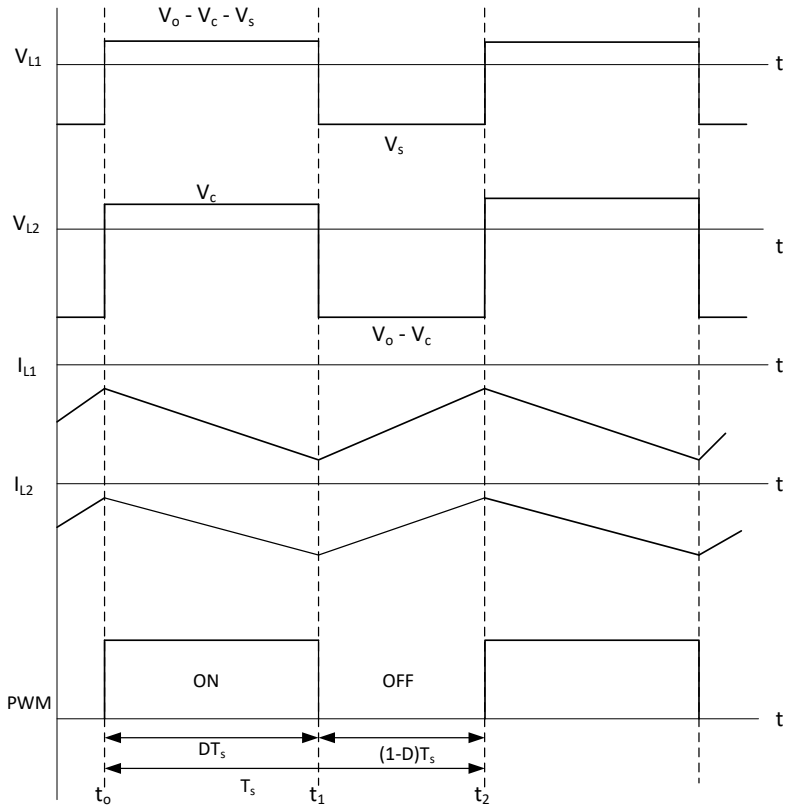

Figure 4.7: The working waveform of converter's operation in step-down mode.

Application of Volt-sec balance principle on indcutor L_1 and L_2 the following equation obtained:

$$D(V_o - V_c - V_s) + (1 - D)(-V_s) = 0 \tag{4.5}$$

$$-DV_c + (1 - D)(V_o - V_c) = 0 \tag{4.6}$$

By eliminating V_c from eq. (4.5) and (4.6) the output voltage of the converter during step-down mode is obtained in eq. (4.7) quadratic in nature.

$$V_s = D^2 V_o \tag{4.7}$$

The voltage across capacitor C_1 is calculated as

$$V_C = DV_o \tag{4.8}$$

4.2.3 Commutation strategy of VSI during regenerative braking

The regenerative braking commutation strategy implemented in this work is the same as that of chapter 3. The three-switch commutation method has already been discussed in section 3.3.3 of chapter 3.

4.3 Converter Design and Stability Analysis

4.3.1 Converter Design

The converter design is done as per its step-up and step-down operations and the converter operates in boundary condition mode for step-up operation. In boundary condition mode the minimum value of inductor L_2 is zero at the beginning of stage-I. The working waveform of the converter in boundary condition is shown in Figure 4.8. In boundary condition operation the current in inductor L_1 is continuous. The inductor's computation is dependent on the current ripple. Let consider the current in inductor L_2 is i_{L2}, thus

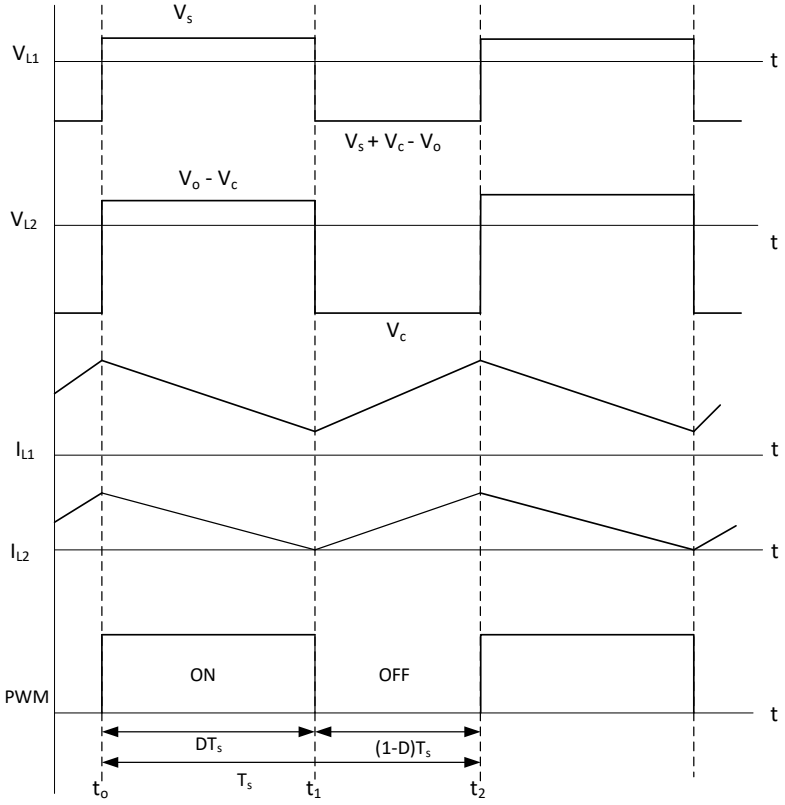

Figure 4.8: Working waveform of converter at boundary condition mode during step-up operation.

the change in current is describe as,

$$\frac{di_{L2}}{dt} = \frac{V_{L2}}{L_2} \tag{4.9}$$

Assuming a linear variation and consider i_{L2_min}=0, the following equation is obtained:

$$\frac{\Delta i_{L2}}{\Delta t} = \frac{i_{L2max} - i_{L2min}}{\Delta t} = \frac{i_{L2max}}{\Delta t} = \frac{V_{L2}}{L_2} \tag{4.10}$$

When the switch S_2 is turned ON, considering Δt= DT_s, T_s=1/f_s, and V_{L2}= V_o-V_c, the maximum current of inductor L_2 is given as:

$$i_{L2max} = \frac{V_0 - V_c}{L_2 f_s} D \tag{4.11}$$

To avoid boundary condition mode, it must be satisfied these condition:

$$i_{L2min} \geq 0 \Rightarrow I_{L2min} \geq I_{L2avg} - \frac{i_{L2max}}{2} \tag{4.12}$$

Substituting (4.3), (4.4) and (4.12) into (4.11), the critical value of inductor L_2 is a function of duty cycle, D

$$L_2 \geq \frac{V_o}{2 I_{L2avg} f_s}(1 - D)D \tag{4.13}$$

Assuming constant output voltage V_o and switching frequency f_s, the value of duty cycle (D) which gives maximum value of L_2. The value of D is obtained by calculating first derivative of (4.13) with respect to D and equals to zero, the D is obtained as 1/2. Therefore the value of L_2 is given as

$$L_2 \geq \frac{V_o}{8 I_{L2avg} f_s} \tag{4.14}$$

Let consider the current in inductor L_1 is i_{L1}, thus the change in current is describe as,

$$\frac{di_{L1}}{dt} = \frac{V_{L1}}{L_1} \tag{4.15}$$

Assuming a linear variation and consider i_{L2_min}=0, the following equation is obtained:

$$\frac{\Delta i_{L1}}{\Delta t} = \frac{i_{L1max} - i_{L1min}}{\Delta t} = \frac{i_{L1max}}{\Delta t} = \frac{V_{L1}}{L_1} \tag{4.16}$$

When the switch S_2 is turned ON, considering Δt= DT_s, T_s=1/f_s, and V_{L1}= V_s, the maximum current of inductor L_1 is given as:

$$i_{L1max} = \frac{V_s}{L_1 f_s} D \tag{4.17}$$

To avoid boundary condition mode, it must be satisfied these condition:

$$i_{L1min} \geq 0 \Rightarrow I_{L1min} \geq I_{L1avg} - \frac{i_{L1max}}{2} \tag{4.18}$$

Substituting (4.4), (4.18) into (4.17), the critical value of inductor L_2 is a function of duty cycle, D

$$L_1 \geq \frac{V_o}{2 I_{L1avg} f_s} D(1 - D)^2 \tag{4.19}$$

The value of D is obtained to maximize L_1 by calculating first derivative of (4.19) with respect to D and equals to zero and Then the value of D is obtained as 1/3.

$$L_1 \geq \frac{2V_o}{27I_{L1avg}f_s} \tag{4.20}$$

Consider linear variation, capacitor C_1 can be calculated based on output current.

$$I_o = C_1\frac{\Delta V_o}{\Delta t} \tag{4.21}$$

$$I_o = I_{L1}(1-D)^2 = I_{L2}(1-D) \tag{4.22}$$

When switch S_2 is turned ON, the value of Δt= DT_s, T_s= $1/f_s$, and using (4.17) the capacitor C_1 is calculated as:

$$C_1 = \frac{DI_o}{\Delta V_o f_s} = \frac{I_{L1avg}}{\Delta V_o f_s}D(1-D)^2 \tag{4.23}$$

The value of D is obtained to maximize C_1 by calculating first derivative of (4.23) with respect to D and equals to zero and Then the value of D is obtained as 1/3.

$$C_1 = \frac{4I_{L1avg}}{27\Delta V_o f_s} \tag{4.24}$$

The value of capacitor C_o is calculated as:

$$I_{co} = C_o\frac{\Delta V_{co}}{\Delta t} \tag{4.25}$$

$$I_{L2} - I_o = C_o\frac{\Delta V_o}{(1-D)T_s} \tag{4.26}$$

$$C_o = \frac{I_{L1avg}}{\Delta V_o f_s}D(1-D)^2 \tag{4.27}$$

The value of duty cycle, D is obtained to maximize C_o by calculating first derivative of (4.27) with respect to D and equals to zero and Then the value of D is obtained as 1/3.

$$C_o = \frac{4I_{L1avg}}{27\Delta V_o f_s} \tag{4.28}$$

The voltage stress on switches S_1, S_2 S_3 and S_4 during step-up and step-down operation of converter are obtained as

$$V_{S1} = V_{S3} = \frac{DV_s}{(1-D)} \tag{4.29}$$

$$V_{S2} = V_{S4} = \frac{V_s}{(1-D)^2} \tag{4.30}$$

The different stage for the discontinuous conduction mode (DCM) in step-up operation are explained below. In DCM, there are four stage, first stage is alike to CCM and no need to explaind it again. In second stage, when all the energy stored in L_2 is transferred to load and current through D_4 become zero at t_2 before next switch S_2 is ON. In third stage, all the energy stored in L_1 is transferred to capacitor C_1 and current through D_3 become zero at t_3 before switch S_1 is ON.

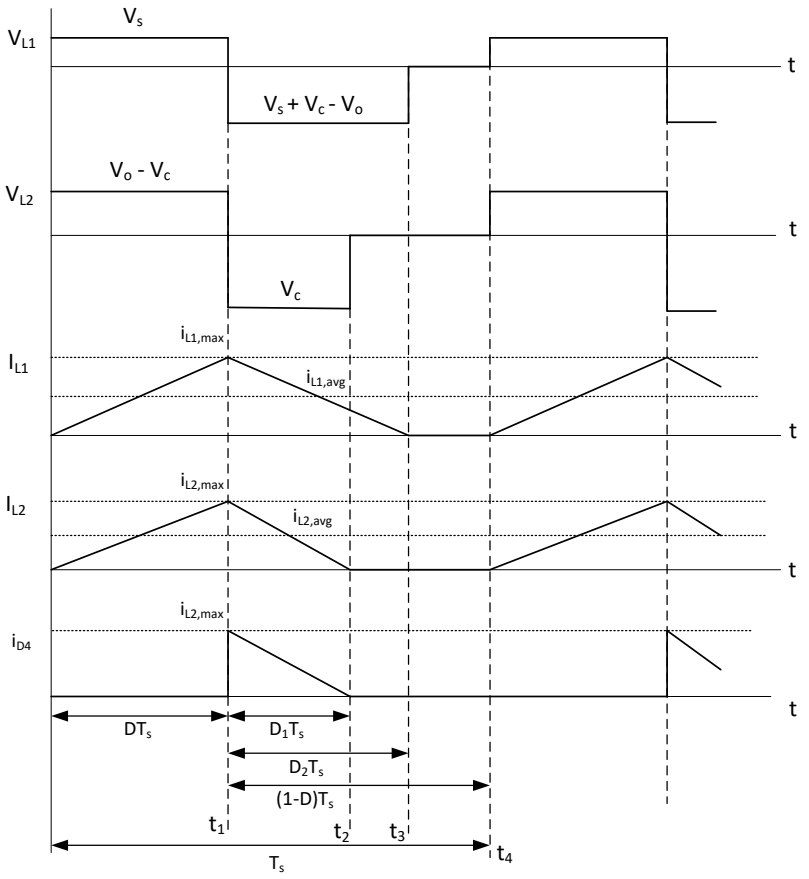

Figure 4.9: Working waveform of converter at DCM during step-up operation.

Figure 4.9 shows the working waveform of the four stages in DCM. As per this, at steady state, the average diode current i_{D4} over one switching period is equal to the $i_{L2,avg}$

$$I_o = i_{D4,avg} = \frac{i_{L2,max}}{2} D_1 \tag{4.31}$$

The voltage across L_1 and L_2 considering step-up and DCM operation

$$DV_s + (1 - D)(V_s + V_c - V_o) = 0 \tag{4.32}$$

$$D(V_c - V_o) + D_1 V_C = 0 \tag{4.33}$$

The voltage gain in DCM is calculated as

$$\frac{V_o}{V_s} = \frac{(D + D_1)}{(D + D_1)(1 - D) + D(D - 1)} \tag{4.34}$$

The equivalent load resistance as R_o and substituting (4.22) into (4.31), and using (4.11) the duty D_1 is given by

$$D_1 = \frac{2L_2 f_s(1 - D)}{R_o D} \tag{4.35}$$

$$D_1 < (1 - D) \tag{4.36}$$

Thus the critical value of the duty cycle to avoid the converter's operation in DCM is given by

$$D > \frac{2L_2 f_s}{R_o} \tag{4.37}$$

4.3.2 Stability Analysis

The stability of any system is define as ability to produce bounded output when a bounded input is applied to it. The general state space representation of an system is given by

$$\dot{x}(t) = Ax(t) + Bu(t) \tag{4.38}$$

$$y(t) = Cx(t) + Du(t) \tag{4.39}$$

The dynamic equation of the converter when Switches S_1 and S_2 are ON in step-up operation is written as

$$-V_s + L_1 \frac{di_{L1}}{dt} = 0 \tag{4.40}$$

$$L_2 \frac{di_{L2}}{dt} - V_{co} + V_c = 0 \tag{4.41}$$

$$C_1 \frac{dV_c}{dt} - i_{L2} = 0 \tag{4.42}$$

$$i_{L2} + C_o \frac{dV_{co}}{dt} + i_o = 0 \tag{4.43}$$

$$V_o = V_{co} \tag{4.44}$$

The state space equation of the converter in step-up for ON condition is

$$\dot{x}(t) = A_1 x(t) + B_1 u(t) \tag{4.45}$$

$$\begin{pmatrix} \dot{i_{L1}} \\ \dot{i_{L2}} \\ \dot{v_c} \\ \dot{v_{co}} \end{pmatrix} = \begin{pmatrix} 0 & 0 & 0 & 0 \\ 0 & 0 & \frac{1}{L_2} & \frac{-1}{L_2} \\ 0 & \frac{1}{C_1} & 0 & 0 \\ 0 & \frac{-1}{C_o} & 0 & \frac{-1}{R_o C_o} \end{pmatrix} \begin{pmatrix} i_{L1} \\ i_{L2} \\ v_c \\ v_{co} \end{pmatrix} + \begin{pmatrix} \frac{1}{L_1} \\ 0 \\ 0 \\ 0 \end{pmatrix} \begin{pmatrix} v_s \end{pmatrix} \tag{4.46}$$

$$y(t) = C_1 x(t) + D_1 u(t) \tag{4.47}$$

$$\begin{pmatrix} v_o \end{pmatrix} = \begin{pmatrix} 0 & 0 & 0 & 1 \end{pmatrix} \begin{pmatrix} i_{L1} \\ i_{L2} \\ v_c \\ v_{co} \end{pmatrix} + \begin{pmatrix} 0 \end{pmatrix} \begin{pmatrix} v_s \end{pmatrix} \tag{4.48}$$

The dynamic equation of the converter when all Switches S_1, S_2, S_3 and S_4 are ON in step-up operation is written as

$$-V_s + L_1 \frac{di_{L1}}{dt} - V_c + V_{co} = 0 \tag{4.49}$$

$$L_2 \frac{di_{L2}}{dt} + V_c = 0 \tag{4.50}$$

$$-i_{L1} - C_1 \frac{dV_c}{dt} + i_{L2} = 0 \tag{4.51}$$

$$C_o \frac{dV_{co}}{dt} + i_o - i_{L1} = 0 \tag{4.52}$$

$$V_o = V_{co} \tag{4.53}$$

The state space equation of the converter in step-up for OFF condition is

$$\dot{x}(t) = A_2 x(t) + B_2 u(t) \tag{4.54}$$

$$\begin{pmatrix} \dot{i_{L1}} \\ \dot{i_{L2}} \\ \dot{v_c} \\ \dot{v_{co}} \end{pmatrix} = \begin{pmatrix} 0 & 0 & \frac{1}{L_1} & \frac{-1}{L_1} \\ 0 & 0 & \frac{-1}{L_2} & 0 \\ \frac{-1}{C_1} & \frac{1}{C_1} & 0 & 0 \\ \frac{1}{C_o} & 0 & 0 & \frac{-1}{R_o C_o} \end{pmatrix} \begin{pmatrix} i_{L1} \\ i_{L2} \\ v_c \\ v_{co} \end{pmatrix} + \begin{pmatrix} \frac{1}{L_1} \\ 0 \\ 0 \\ 0 \end{pmatrix} \begin{pmatrix} v_s \end{pmatrix} \tag{4.55}$$

$$y(t) = C_1 x(t) + D_1 u(t) \tag{4.56}$$

$$\begin{pmatrix} v_o \end{pmatrix} = \begin{pmatrix} 0 & 0 & 0 & 1 \end{pmatrix} \begin{pmatrix} i_{L1} \\ i_{L2} \\ v_c \\ v_{co} \end{pmatrix} + \begin{pmatrix} 0 \end{pmatrix} \begin{pmatrix} v_s \end{pmatrix} \tag{4.57}$$

Now applying state-space averaging technique

$$A = A_1 D + A_2(1-D) \tag{4.58}$$

$$B = B_1 D + B_2(1-D) \tag{4.59}$$

$$A = \begin{pmatrix} 0 & 0 & \frac{(1-D)}{L_1} & \frac{-(1-D)}{L_1} \\ 0 & 0 & \frac{-1}{L_2} & \frac{D}{L_2} \\ \frac{-(1-D)}{C_1} & \frac{1}{C_1} & 0 & 0 \\ \frac{(1-D)}{C_o} & \frac{(-D)}{C_o} & 0 & \frac{-1}{R_o C_o} \end{pmatrix} \tag{4.60}$$

$$B = \begin{pmatrix} \frac{1}{L_1} \\ 0 \\ 0 \\ 0 \end{pmatrix} \tag{4.61}$$

$$C = \begin{pmatrix} 0 & 0 & 0 & 1 \end{pmatrix} \tag{4.62}$$

$$D = \begin{pmatrix} 0 \end{pmatrix} \tag{4.63}$$

Small signal model is derived by applying perturbations, the overall state and output equation of the converter is obtained as

$$\begin{pmatrix} \widetilde{i_{L1}} \\ \widetilde{i_{L2}} \\ \widetilde{v_c} \\ \widetilde{v_{co}} \end{pmatrix} = \begin{pmatrix} 0 & 0 & \frac{(1-D)}{L_1} & \frac{-(1-D)}{L_1} \\ 0 & 0 & \frac{-1}{L_2} & \frac{D}{L_2} \\ \frac{-(1-D)}{C_1} & \frac{1}{C_1} & 0 & 0 \\ \frac{(1-D)}{C_o} & \frac{-D}{C_o} & 0 & \frac{-1}{R_o C_o} \end{pmatrix} \begin{pmatrix} \widetilde{i_{L1}} \\ \widetilde{i_{L2}} \\ \widetilde{v_c} \\ \widetilde{v_{co}} \end{pmatrix} + \begin{pmatrix} \frac{v_{co}-v_c}{L_1} & \frac{1}{L_1} \\ \frac{v_{co}}{L_2} & 0 \\ \frac{i_{L1}}{C_1} & 0 \\ \frac{-(i_{L1}-i_{L2})}{C_o} & 0 \end{pmatrix} \begin{pmatrix} \widetilde{d} \\ \widetilde{v_s} \end{pmatrix} \tag{4.64}$$

After substituting all passive elements value from Table 4.1 and duty cycle D = 0.51, control to output transfer function *G(s)* is obtained as follows

$$G_d(s) = \frac{\widetilde{v_o(s)}}{\widetilde{d(s)}} = \frac{-3.46 \times 10^5 s^3 + 5.38 \times 10^8 s^2 - 5.45 \times 10^{12} s + 2.42 \times 10^{16}}{1.11 s^4 + 2.8 \times 10^2 s^3 + 4.4 \times 10^7 s^2 + 8.6 \times 10^9 s + 2.96 \times 10^{13}} \tag{4.65}$$

From the above transfer function, it is observed that the all the poles and two zeros lies on left half and one zero lies on right half of S-plane of in root locus. Transfer function of a PI controller is

$$G_{PI} = \frac{K_p s + K_i}{s} \tag{4.66}$$

Ziegler-Nicolous' closed loop method is used to tune the PI controller, the value of $K_p = 1.93 \times 10^{-4}$ and $K_i = 0.172$ substituted in (4.66) and therefore the closed loop transfer

function (CLTF) of the converter is obtained as follows

$$CLTF = \frac{\widetilde{v_o(s)}}{\widetilde{v_{ref}(s)}} = \frac{-66.91s^4 + 4.42 \times 10^4 s^3 - 9.6 \times 10^8 s^2 + 3.73 \times 10^{12} s + 4.16 \times 10^{15}}{s(1.11s^4 + 2.8 \times 10^2 s^3 + 4.4 \times 10^7 s^2 + 8.6 \times 10^9 s + 2.96 \times 10^{13})} \tag{4.67}$$

The magnitude and phase plot is obtained from CLTF are shown in Figure 4.10. In magnitude plot there two up-down glich, it occours due to two pair of complex conjugate pole ($P_{1,2}$= -26.8 ± j6243, $P_{3,4}$= -99.1 ± j821) and one pair of conjugate zero ($Z_{1,2}$= -860 ± j4544) in the open loop transfer function *G(s)* of the converter. From bode diagram one can see phase margin (PM=40.8^0) and gain margin (GM=2.81 dB) so it can say that the system is stable.

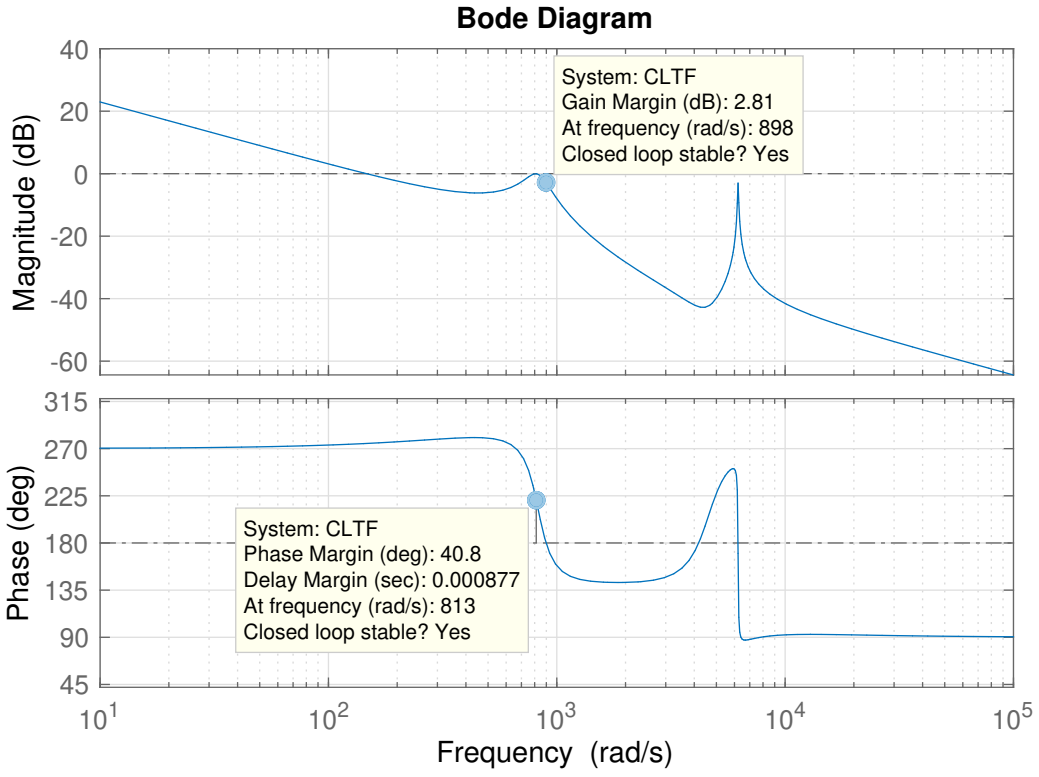

Figure 4.10: Mganitude and phase plot is obtained from CLTF.

4.4 Computational and Experimental results

4.4.1 Computational Results

System at Output Voltage 200 V and operating frequency 20 kHz

The bidirectional quadratic converter along with VSI for the PMBLDC machine is simulated in MATLAB/Simulink. The vehicular load is simulated through a drum-belt during motoring operation and an inertial load of 0.1 kg-m^2 during regenerative braking operation. The proposed converter is simulated and designed for 1 kW power at an output voltage of 200 V with battery voltage at 48 V and switching frequency of 20 kHz. The parameters of the converter are calculated and its value is given in Table 4.1. The Pulse

Table 4.1: Converter specifications.

Parameter	Value
Input voltage (V_s)	48 V
Output power (P_o)	1 kW
Output voltage (V_o)	200 V
Switching frequency (f_s)	20 kHz
Inductor (L_1, L_2)	0.37 mH, 1.25 mH
Capacitor (C_1, C_o)	47 μF, 100 μF
Switches S_1-S_4	STWA63N65DM2

width modulation (PWM) signal to turn ON the switches of the proposed converter are generated in MATLAB/Simulink is shown in Figure 4.11. One can see that the switching frequency of the PWM is 20 kHz. The PWM signal of VSI for PMBLDC motor are generated based on position of the rotor which is sensed by hall sensors. The PWM signal of VSI is illustrated in Figure 4.12. The system is simulated for 6s with 0s to 4s in step-up (motoring) and 4s to 6s in step-down RB mode. In step-up when switches S_1 and S_2 are ON, the inductor currents I_{L1}, I_{L2} increases and when switches S_1 and S_2 are OFF, the inductor currents I_{L1}, I_{L2} decreases. The steady-state inductor currents I_{L1} and I_{L2} are shown in Figure 4.13 during the step-up operation of the converter. At time t=4s, regenerative braking is applied, the proposed converter is operating in step-down mode, and the energy stored in an inertial flywheel is fed back to back by boosting the back

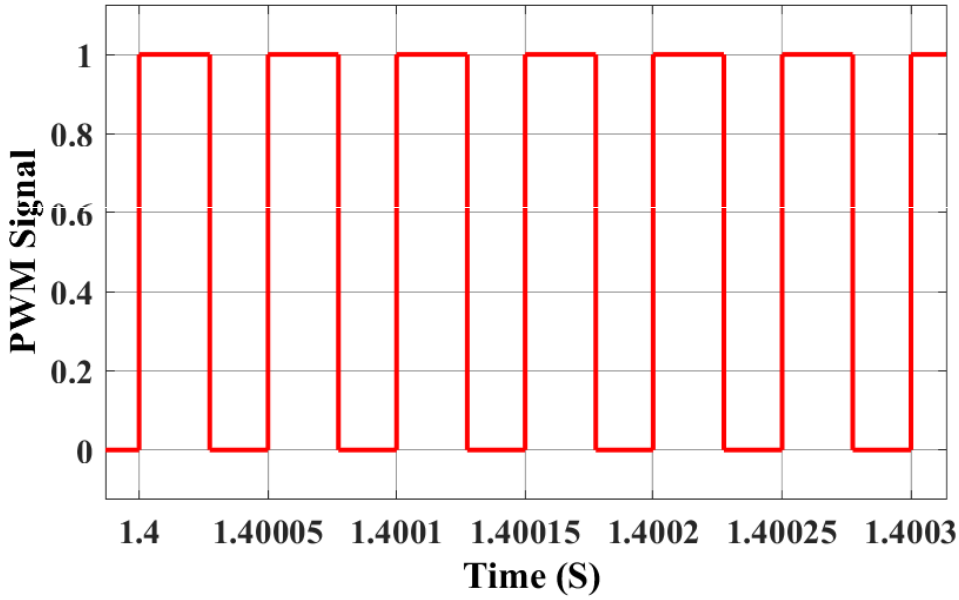

Figure 4.11: The PWM signal for switches of the proposed converter in MATLAB/Simulink.

EMF using self-inductance of the PMBLDC motor. The inductor currents are negative during step-down or regenerative braking operation of the converter. In step-down RB operation of the converter, switches S_3 and S_4 are ON. When switches S_3 and S_4 are ON, inductor currents I_{L1} and I_{L2} are increases and When switches S_3 and S_4 are OFF, the inductor currents I_{L1} and I_{L2} are decreased. The steady-state inductor currents during step-down mode are shown in Figure 4.14.

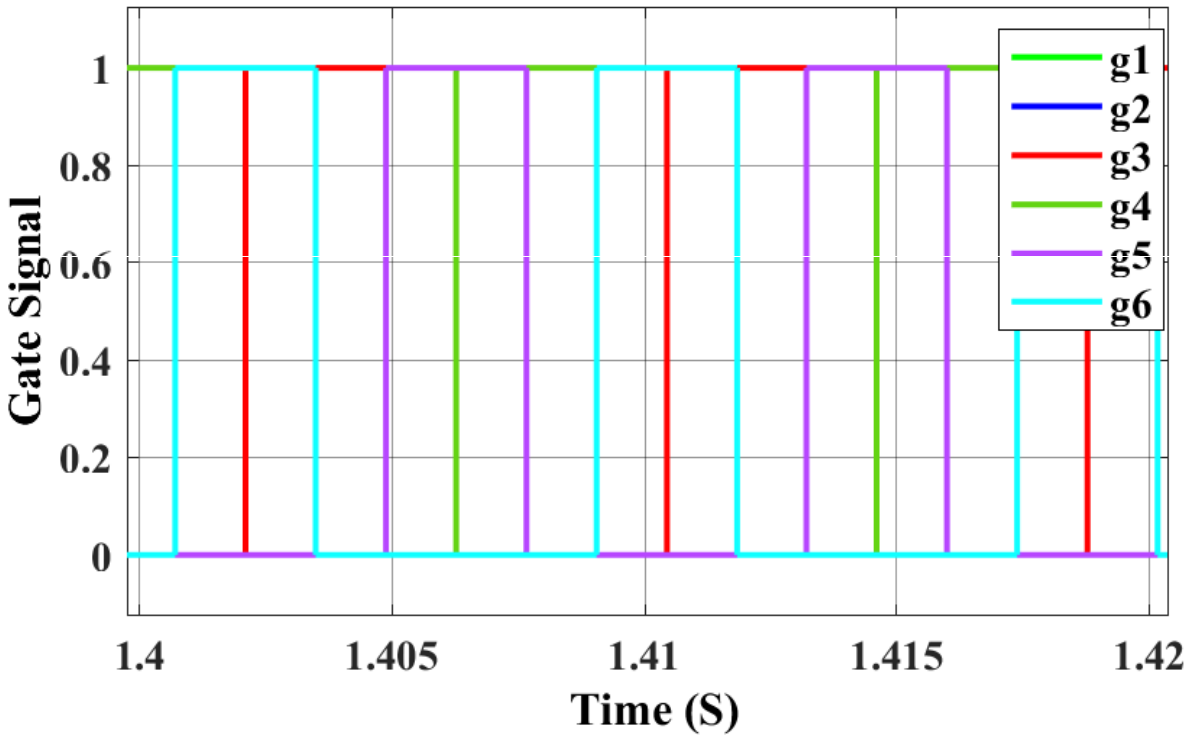

Figure 4.12: The PWM signal of VSI for PMBLDC motor in MATLAB/Simulink.

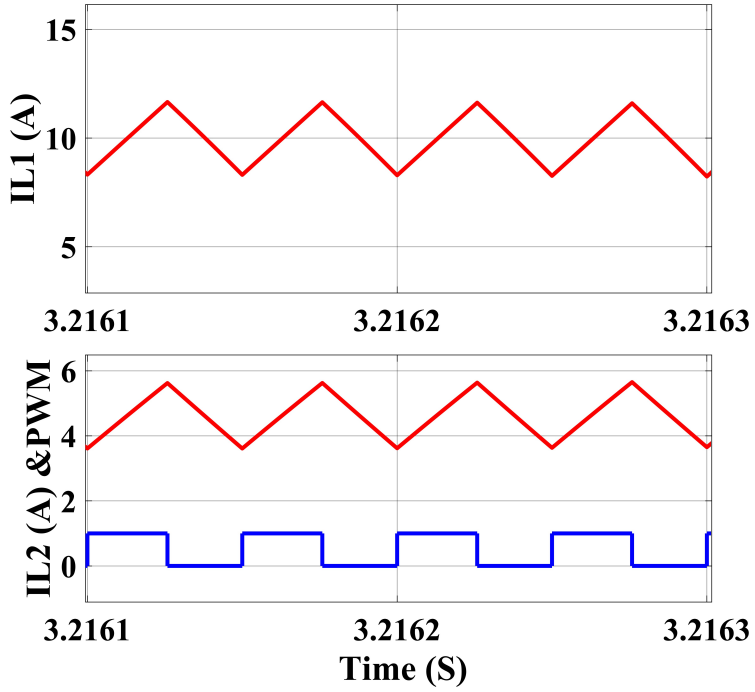

Figure 4.13: The steady-state inductor currents I_{L1} and I_{L2} with switching PWM in step-up operation of the converter.

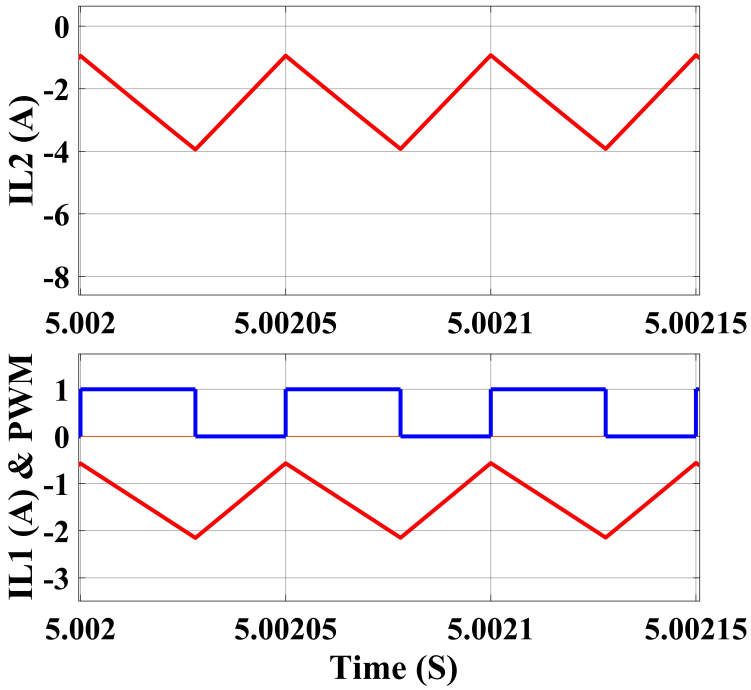

Figure 4.14: The steady-state inductor currents I_{L1} and I_{L2} with switching PWM in step-down operation of the converter.

The steady-state output voltage V_o, capacitor C_1 voltage V_c, and battery voltage V_s during step-up operation of converter are shown in Figure 4.15. One can see that, the battery voltage $V_s = 48$ V, capacitor voltage $V_c = 102$ V and output $V_o = 200$ V in the Figure 4.15. The voltage control is applied to maintained the output voltage at 200 V irrespective of the load by PI controller. The voltage stress on switches S_1 and S_2 during converter's step-up operation are shown in Figure 4.16. From Figure 4.16 one can see that the voltage stress on S_1 is $V_{s1} = 100$ V and voltage stress on switch S_2 is $V_{s2} = 200$ V. The voltage stress on switches S_1 and S_3 are equal and similarly voltage stress on switches S_2 ans S_4 are equal.

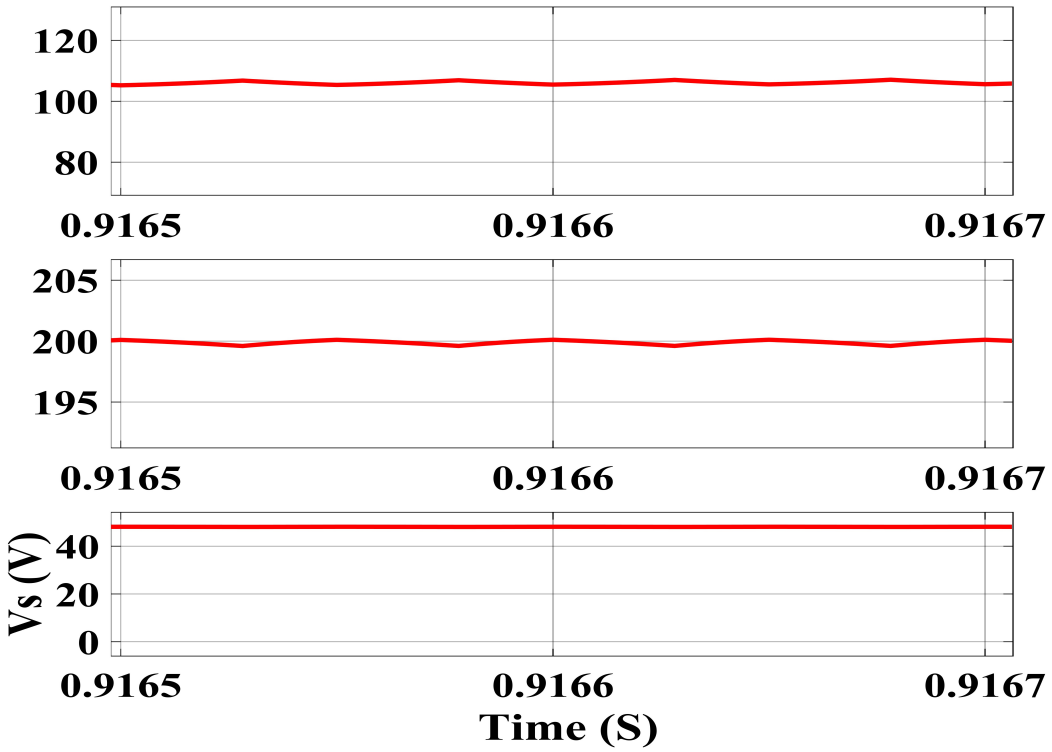

Figure 4.15: The steady-state output voltage, input voltage and capacitor voltage during step-up operation of the converter.

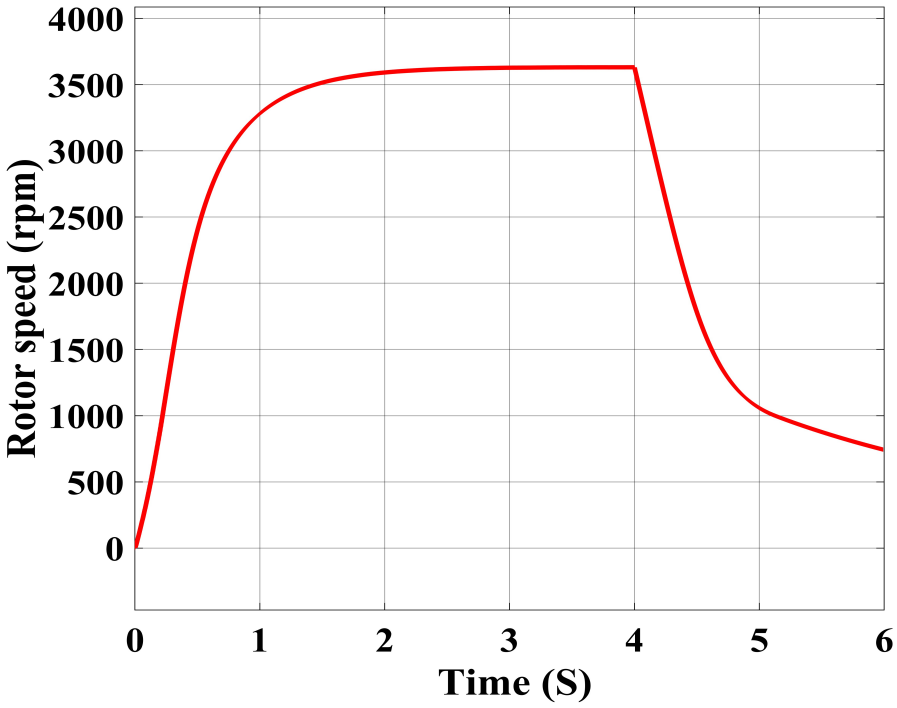

Figure 4.17: PMBLDC motor speed characteristics during motoring and regenerative braking.

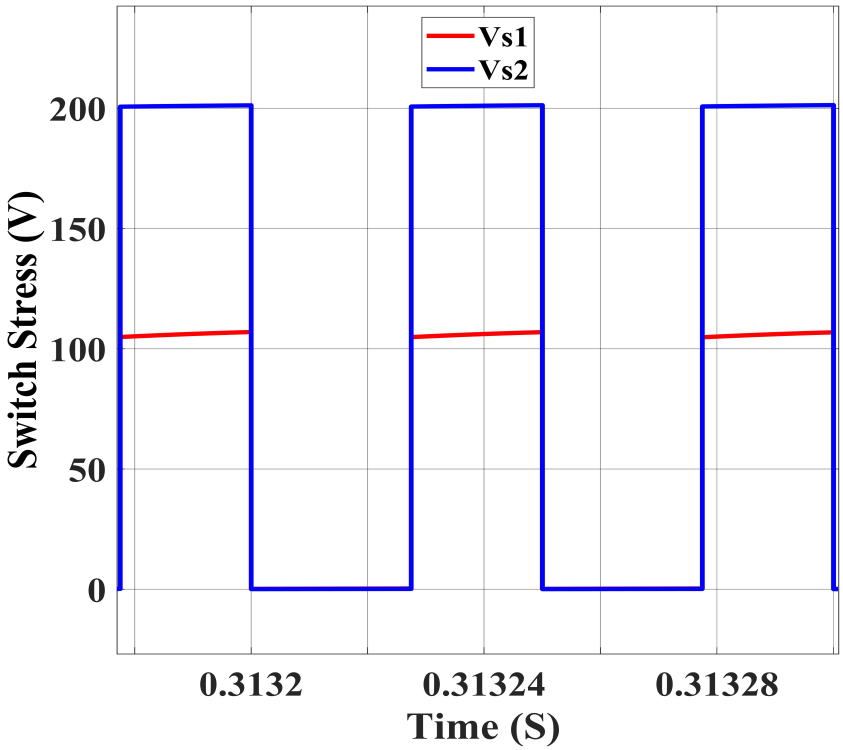

Figure 4.16: Voltage stress on switches S_1 and S_2 in step-up operation of the converter.

The speed characteristics of PMBLDC machine during motoring from time 0s to 4s, the speed reached at 3600 rpm and at time 4s RB is applied the speed reduced from 3600 rpm to 600 rpm one can see in Figure 4.17. The three phase stator current of PMBLDC motor in motoring mode operation are shown in Figure 4.18. The three phase stator current of PMBLDC motor in regeneartive braking mode operation are shown in Figure 4.19.

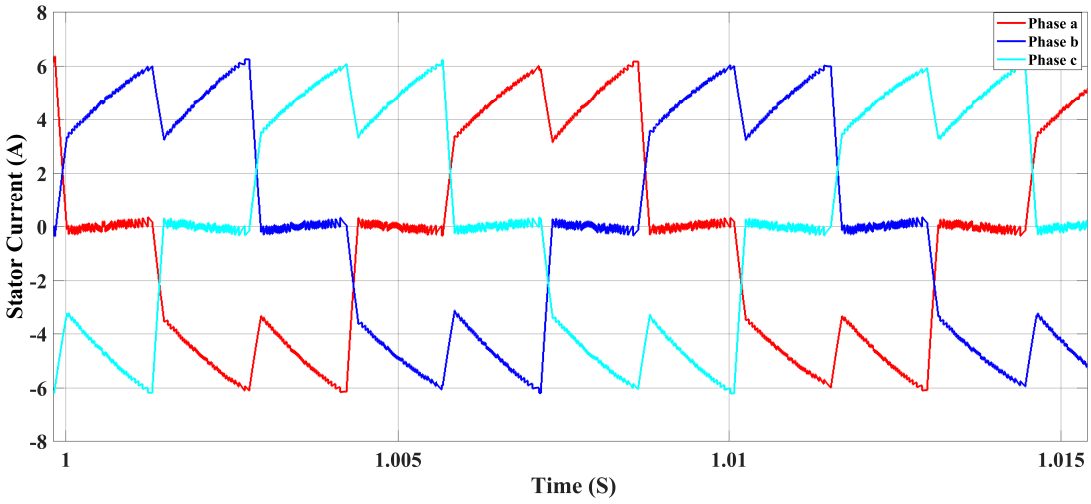

Figure 4.18: Three phase stator current of PMBLDC motor in motoring mode.

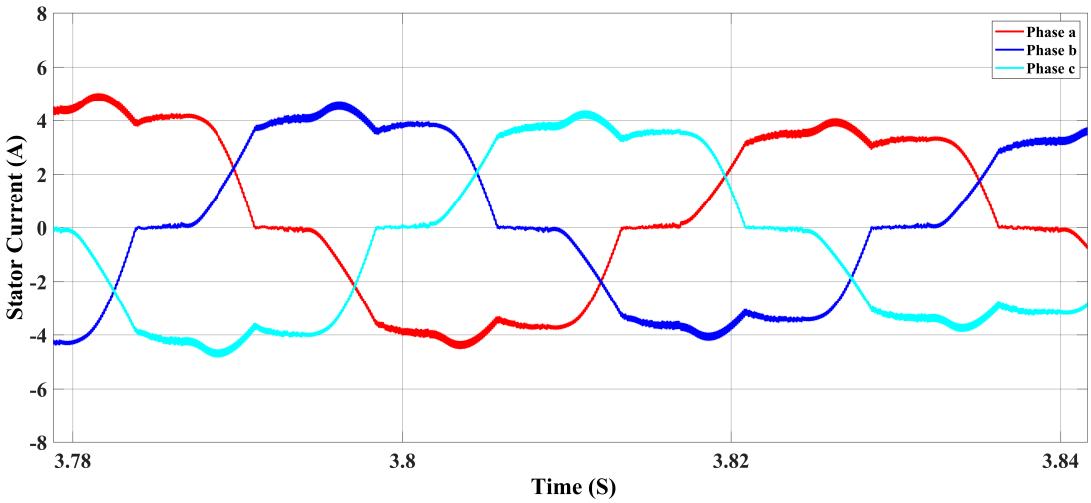

Figure 4.19: Three phase stator current of PMBLDC motor in regenerative braking mode.

System at Output Voltage 98 V and Operating Frequency 15 kHz

The bidirectional quadratic converter along with VSI for the PMBLDC machine is simulated in MATLAB/Simulink. The vehicular load is simulated through a drum-belt during motoring operation and an inertial load of 0.1 kg-m^2 during regenerative braking operation. The converter is simulated and designed for 1 kW power at an output voltage of 98 V with battery voltage at 48 V and switching frequency of 15 kHz. The parameters of the converter are calculated and its value is given in Table 4.2. The working of the converter

Table 4.2: Converter specifications.

Parameter	Value
Input voltage (V_s)	48 V
Output power (P_o)	1 kW
Output voltage (V_o)	98 V
Switching frequency (f_s)	15 kHz
Inductor (L_1, L_2)	0.47 mH, 1.6 mH
Capacitor (C_1, C_o)	47 μF, 100 μF
Switches S_1-S_4	STWA63N65DM2

at output voltage 98 V, frequency 15 kHz is same as that of output of voltage 200 V and frequency 20 kHz.

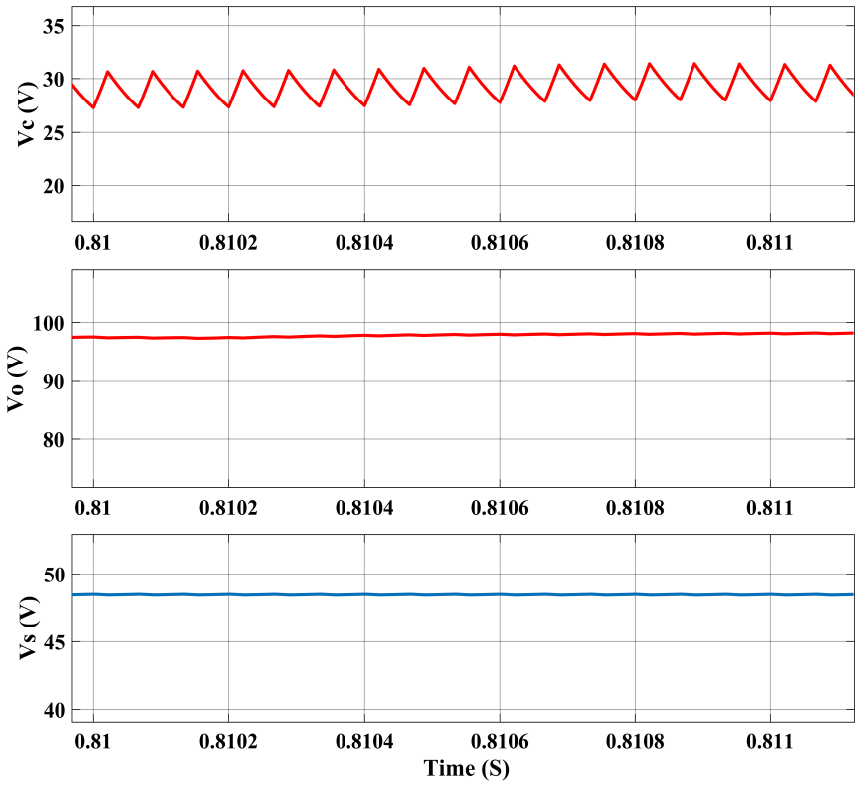

Figure 4.20: Capacitor Voltage V_c, output voltage V_o and input voltage V_s during step-up operation.

The simulation results of different parameters are illustrated. The voltage across

capacitor C_1 (V_c), output voltage V_o and input voltage V_s are shown in Figure 4.20. The Inductors current I_{L1}, I_{L2} with switching PWM under steady-state during step-up operation are illustrated in Figure 4.21.

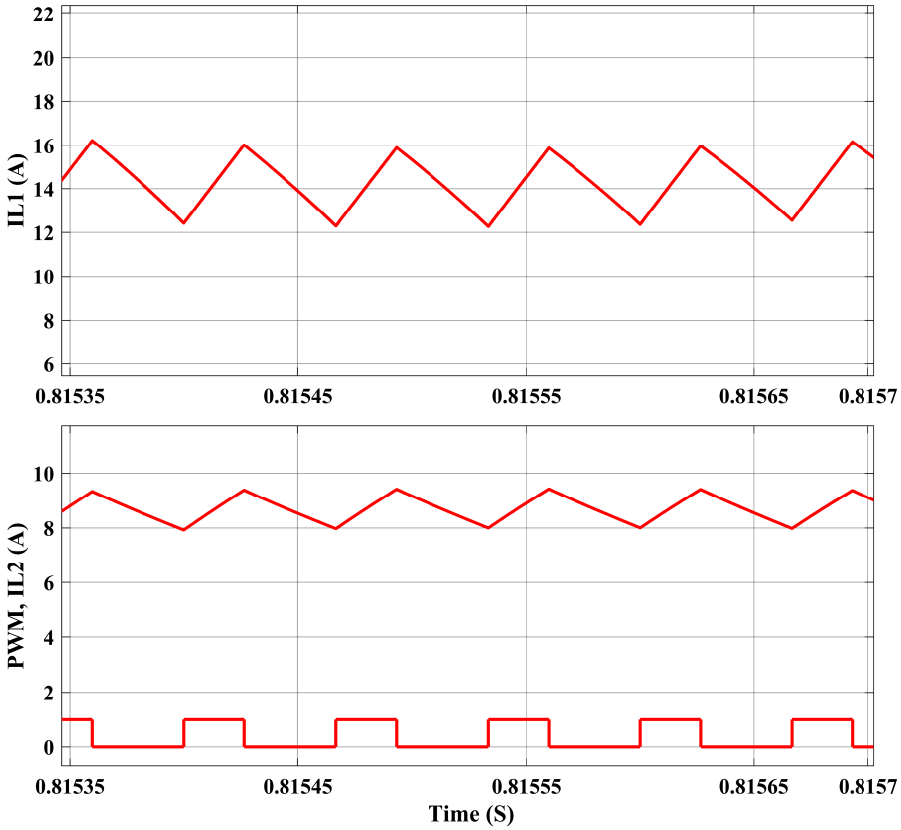

Figure 4.21: Inductors current I_{L1}, I_{L2} with switching PWM under steady-state during step-up operation.

The voltage stress on switches S_1, S_2 with switching PWM are shown in Figure 4.22. As the voltage stress on V_{S1}=V_{S3}=70 v and V_{S2}=V_{S4}=98 V therefore only two switches voltage stress are given in Figure 4.22. The steady-state inductor current with switching PWM during regenerative braking or step-down operation of converter are shown in Figure 4.23.

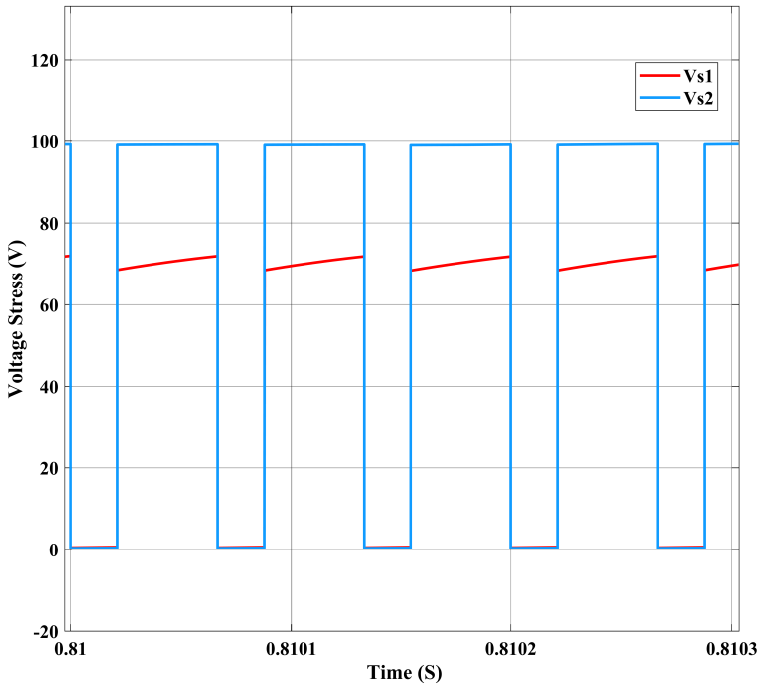

Figure 4.22: Voltage stress on switches S_1 (V_{s1}) and S_2 (V_{s2}) during step-up operation.

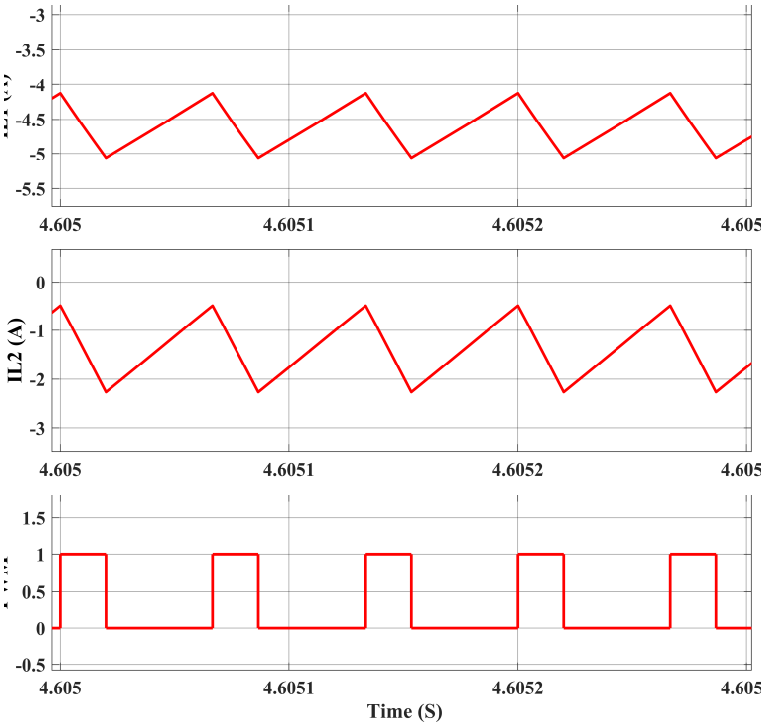

Figure 4.23: Inductor current I_{L1}, I_{L2} with switching PWM during step-down operation of converter.

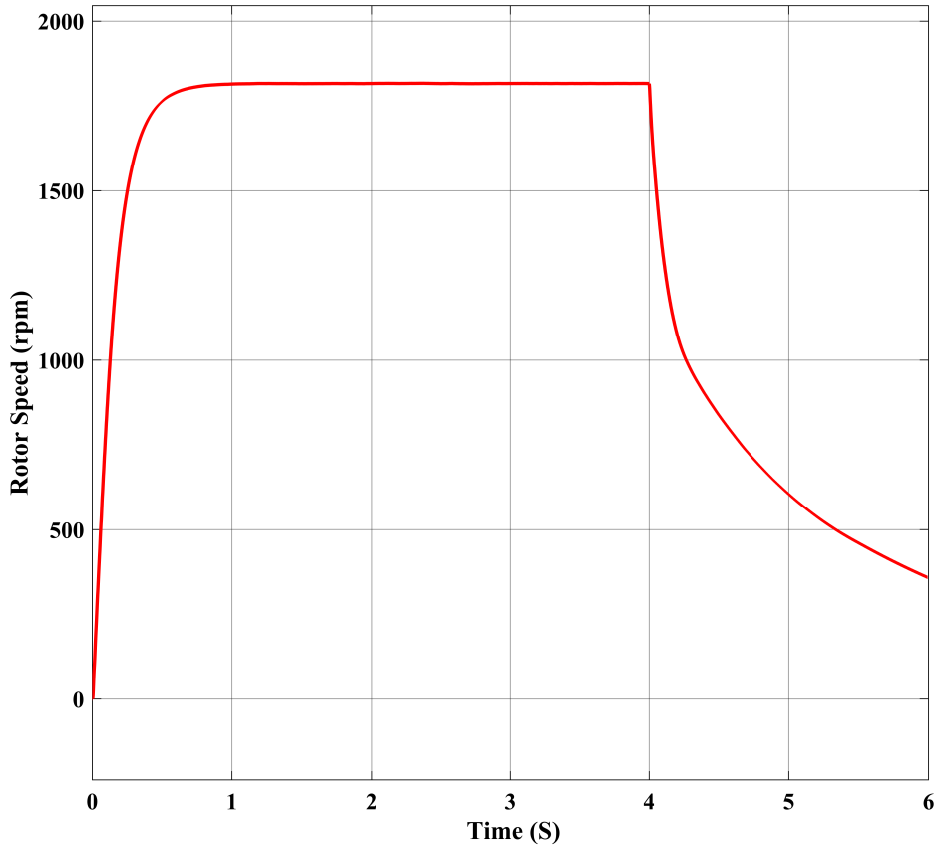

Figure 4.24: PMBLDC motor speed characteristics.

The simulation is run for 6s, from 0s to 4s motoring mode and 4s to 6s regenerative braking mode. The PMBLDC motor speed characteristics is illustrated in Figure 4.24.The speed during motoring reached around 1800 rpm and when RB is applied at t= 4s, speed start decreasing and reached to 400 rpm at t= 6s as seen from Figure 4.24.

4.4.2 Hardware Results

System at Output Voltage 200 V and Operating Frequency 20 kHz

A model of the proposed converter is designed and developed for the experimental validation as shown in Figure. 4.25. The converter component's values used in the prototype are the same as chosen in simulation parameters. The control strategy is realized by using the TMS320F28335 DSP microcontroller for the proposed converter and driving PMBLDC machine in both motoring and RB. A PMBLDC machine is coupled with a flywheel is used to emulate the RB action. To reduce the impulse torque condition and safety of the

system, a pulley belt system is employed for mechanical coupling of the motor and inertial load. The steady-state capacitor voltage V_c, output voltage V_o, and battery voltage V_s during step-up operation of the converter are illustrated in Figure 4.26.

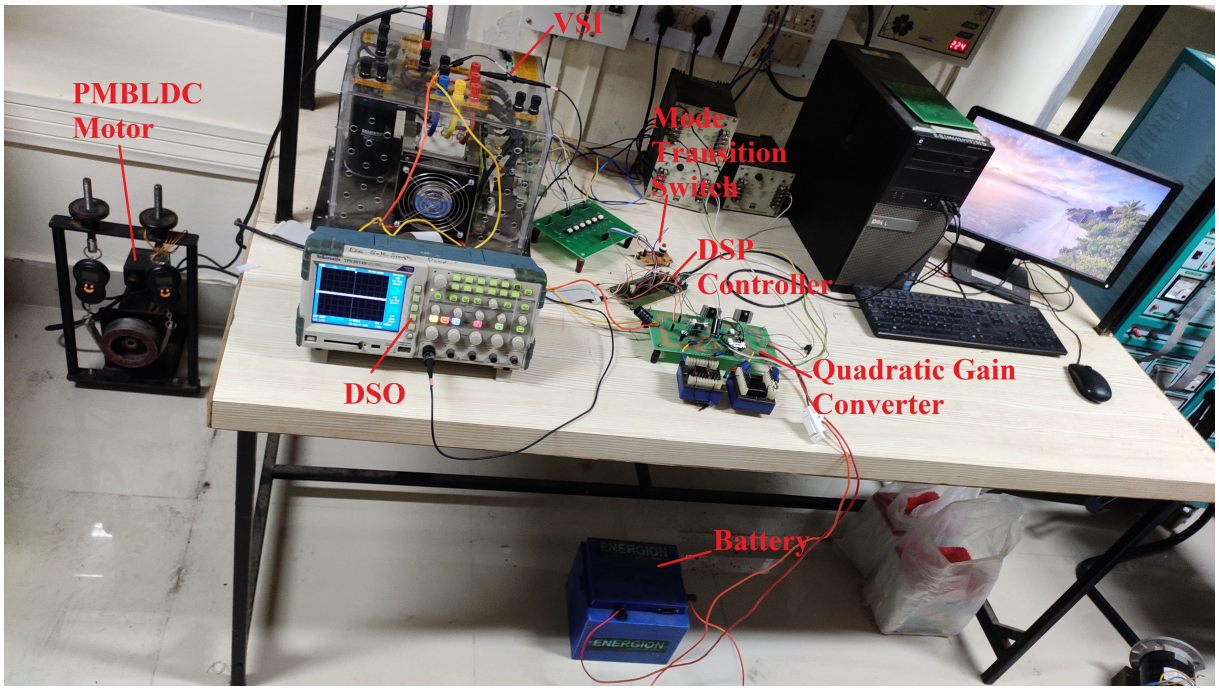

Figure 4.25: Experimental setup.

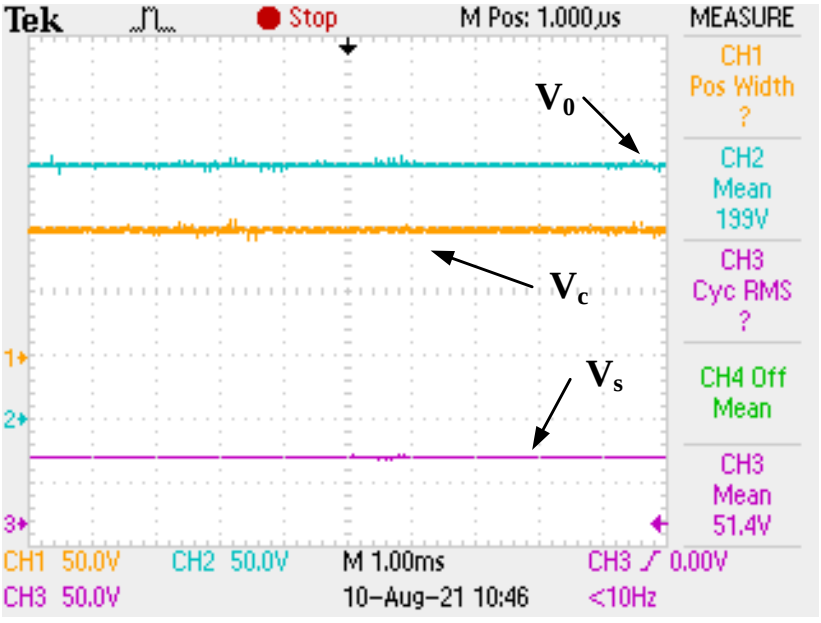

Figure 4.26: The capacitor voltage V_c, ouput voltage V_o, and battery voltage V_s during step-up operation.

The steady-state output voltage (V_o), inductors current I_{L1} and I_{L2} during step-up operation of converter are shown in Figure 4.27. Both the inductors are charging during the ON time of the switch and discharging during the OFF time.

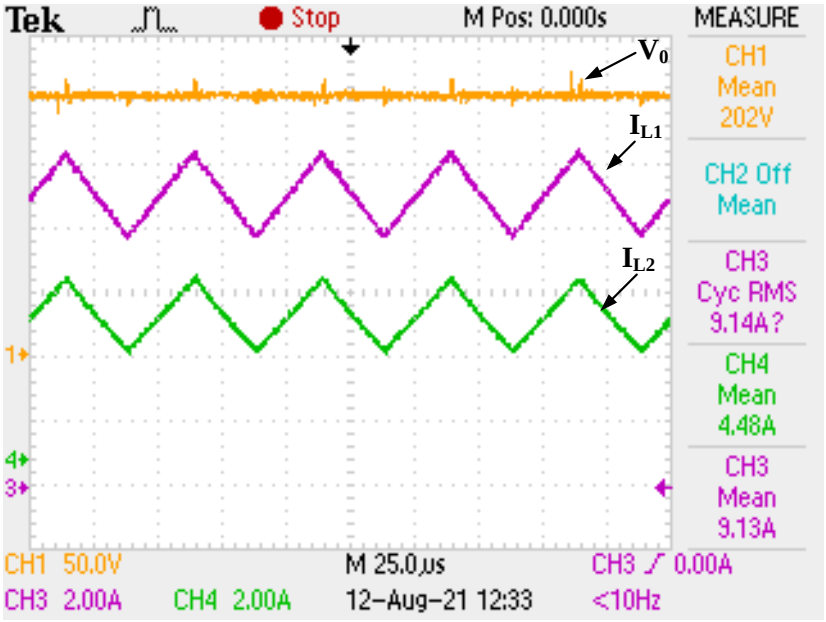

Figure 4.27: The output voltage (V_o), Inductor's current I_{L1}, and I_{L2}.

The converter are operates in different condition depending upon the nature of inductor current during step-up mode. The inductor current at discontinuous condition mode and boundary condition mode are shown in Figure 4.28 and 4.29 respectively.

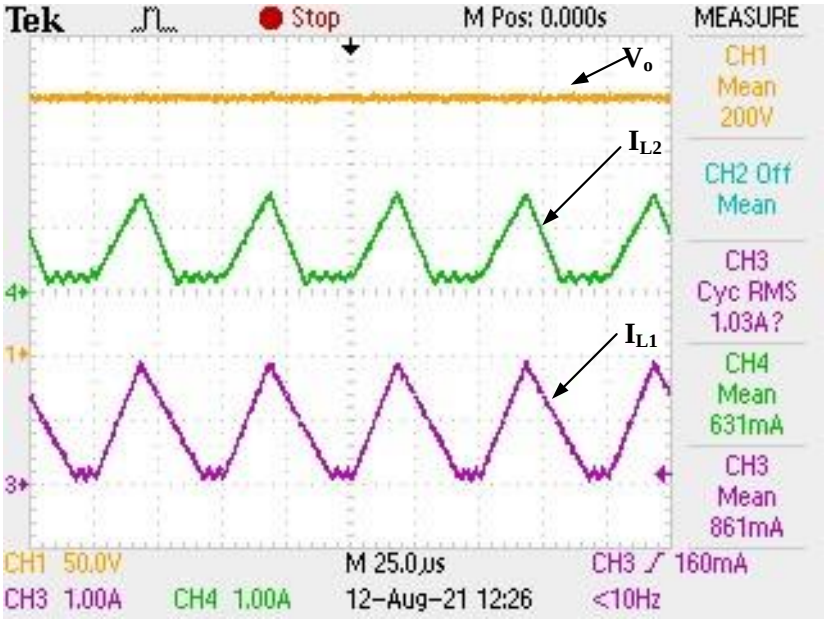

Figure 4.28: Inductor's current I_{L1}, I_{L2}, and output voltage V_o in discontinuous conduction mode.

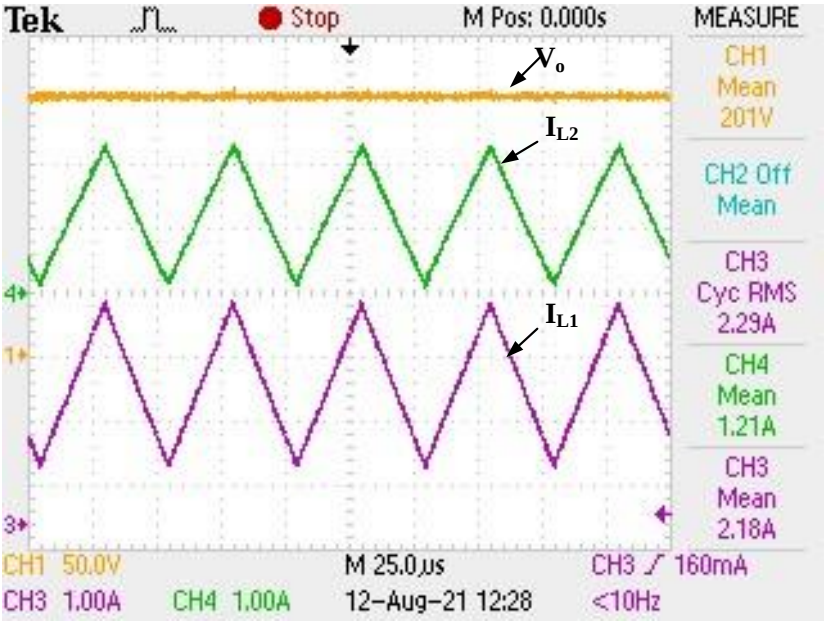

Figure 4.29: Output voltage V_o, inductor's current I_{L1}, and I_{L2} in boundary condition mode.

The PMBLDC machine is coupled with a drum-belt in order to apply load torque, which is connected through a digital weighing machine at both ends. The steady-state three-phase stator current of PMBLDC machine in motoring mode during converter's

step-up operation are shown in Figure 4.30. The voltage stress on switches S_1 and S_2 during step-up operation of the converter are illustrated in Figure 4.31.

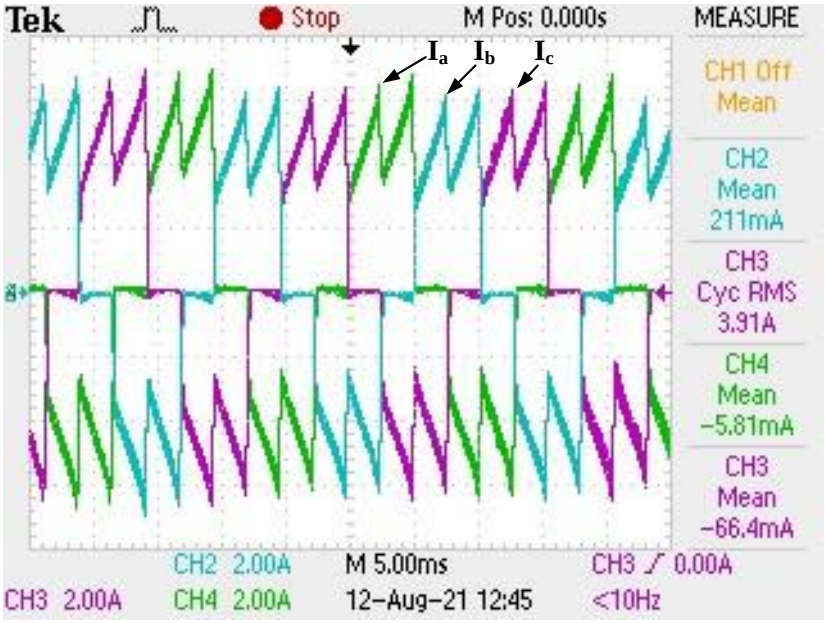

Figure 4.30: Steady-state three phase stator current of PMBLDC machine in motoring mode.

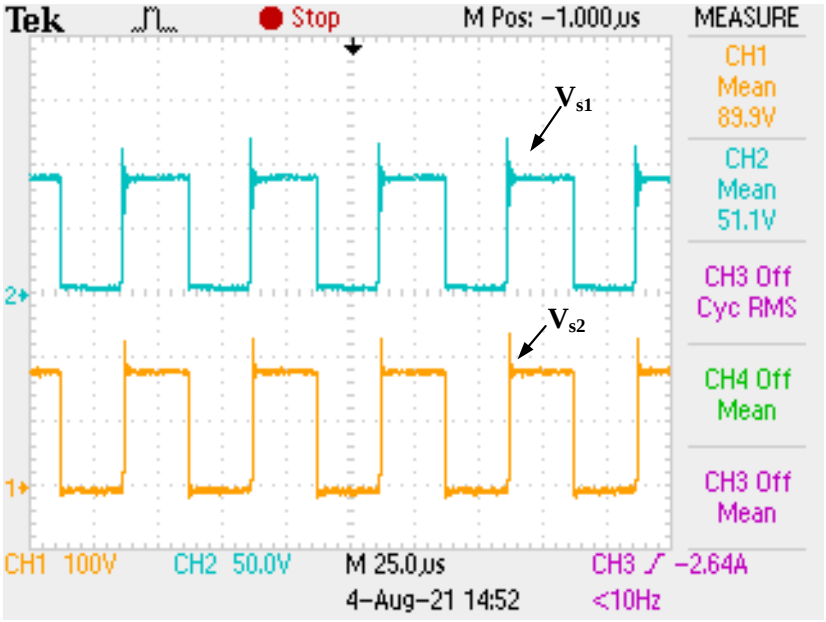

Figure 4.31: Plot of voltage stress on Switches S_1 (V_{s1}) and S_2 (V_{s2}).

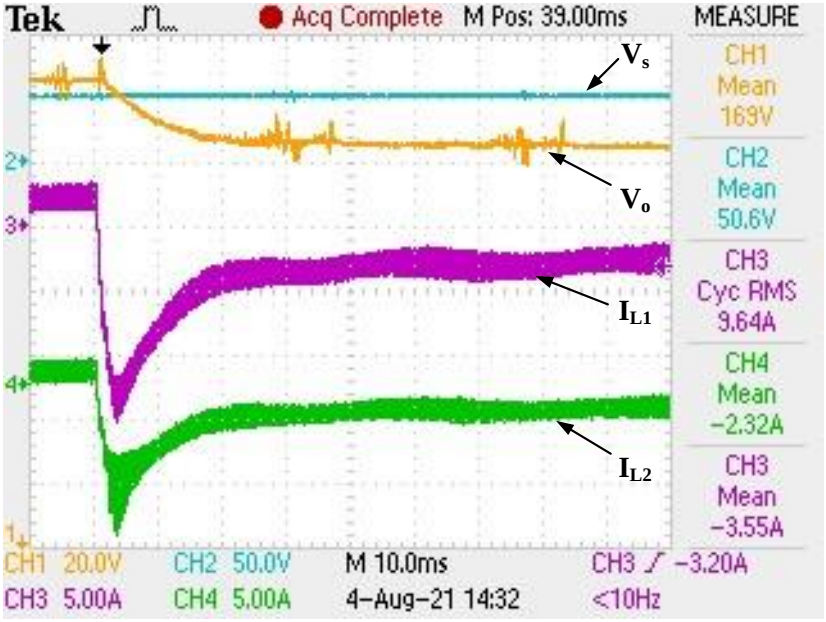

Figure 4.32: The transition of output voltage V_o, battery voltage (V_s), inductor currents I_{L1}, and I_{L2} when RB is applied.

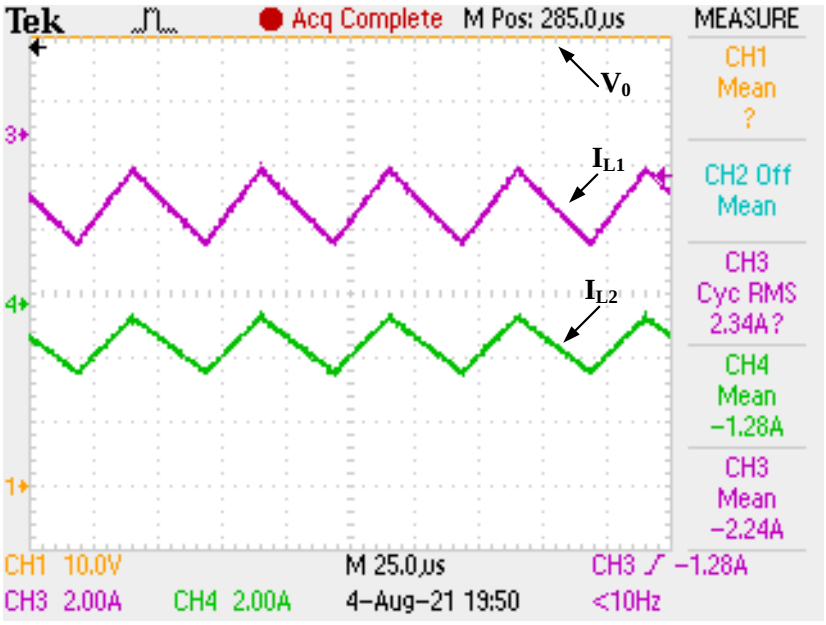

Figure 4.33: Steady-state inductor currents I_{L1} and I_{L2} during step-down operation of converter.

In the step-down or regenerative braking operation of the converter, the PMBLDC machine is loaded with a flywheel to show the power flow from load to battery during RB. A physical mode transition switch is used to change the mode of operation from motoring to RB and vice-versa. When RB is applied through the mode transition switch,

the change in the inductor's current from positive to negative and output voltage of the converter are shown in Figure 4.32. The negative current of the inductor currents implies that the power is flowing from load to source.

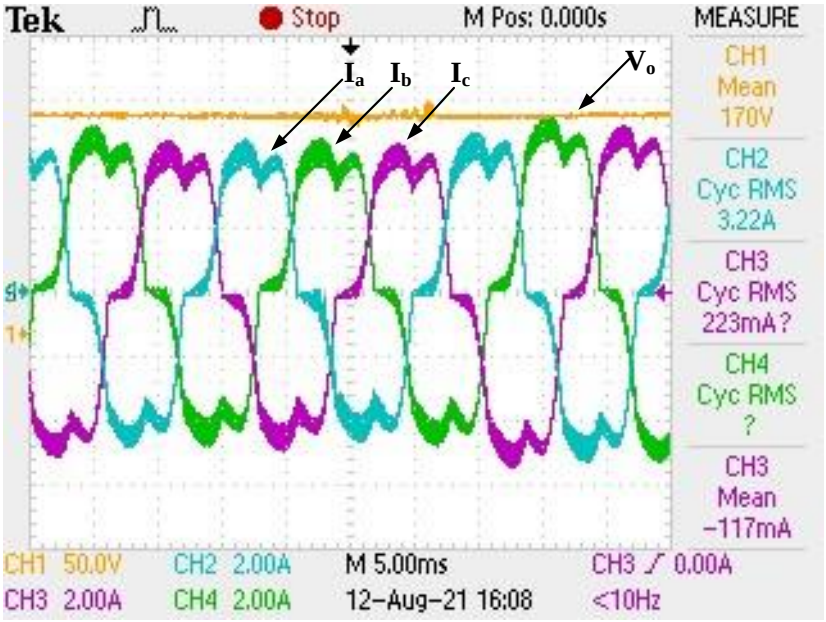

Figure 4.34: Three phase stator current I_a, I_b, I_c, and output voltage V_o during regenerative braking.

The steady-state inductor currents I_{L1} and I_{L2} during step-down operation of the converter and it is negative as shown in Figure 4.33. During regenerative braking, the PMBLDC motor will act as a generator and the three-phase stator current during regenerative braking is shown in Figure 4.34. The stator current in regenerative braking mode has less ripple as compared to the stator current in the motoring mode of operation. So that the PMBLDC machine has better performance in regenerative braking mode. The three-switch control strategy of VSI for RB of PMBLDC motor is done at different braking duty. The braking duty is varied from 0.4 to 0.7, the armature current, battery current, battery voltage, and command signal for RB action is illustrated in Figure 4.35. When the command signal is high, the PMBLDC motor acts in motoring operation and when the command signal goes low, the PMBLDC motor act as a generator in RB. One can see that as braking duty increases then the armature current, battery charging current, and braking torque increase.

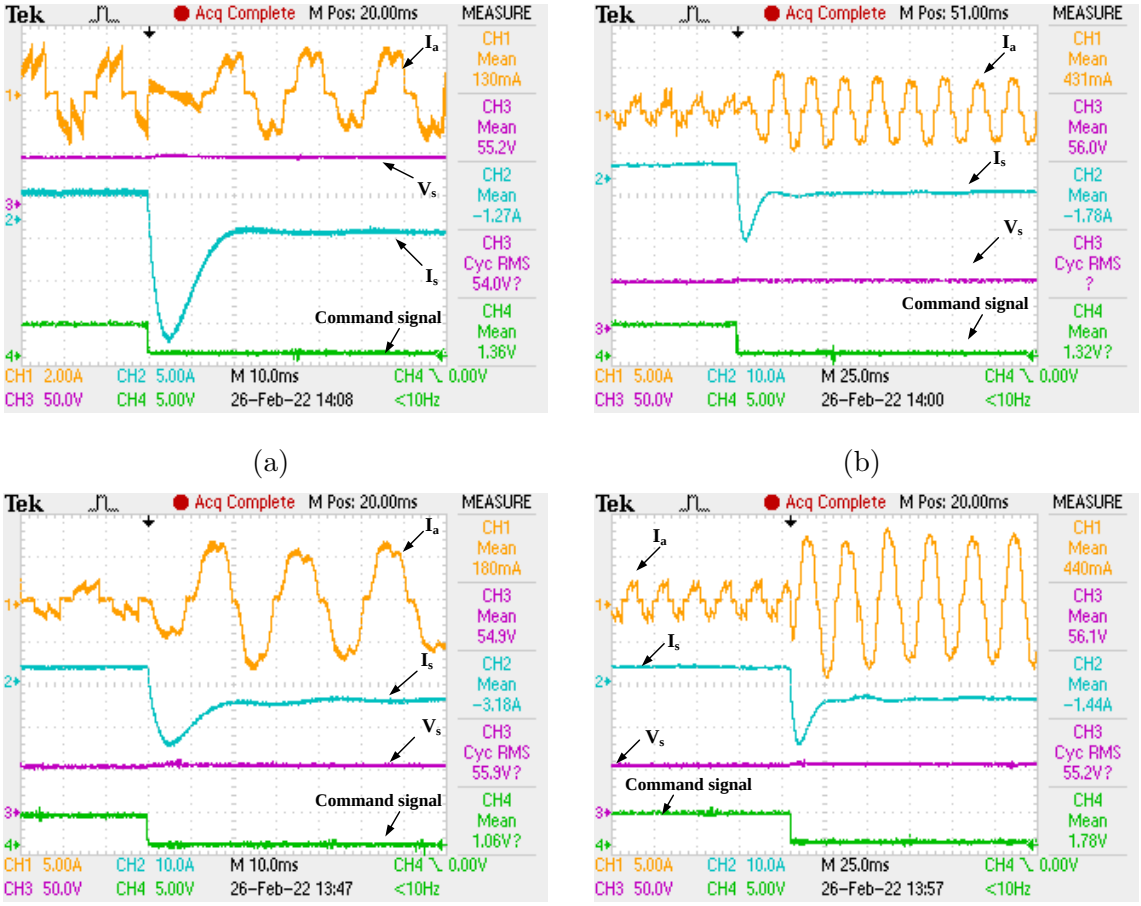

Figure 4.35: Armature current, battery current, battey voltage, command signal at different braking duty (a) $\delta = 0.4$ (b) $\delta = 0.5$ (c) $\delta = 0.6$ and (d) $\delta = 0.7$.

System at Output Voltage 98 V and Operating Frequency 15 kHz

The experimental results are obtained from developed experimental set-up as shown in Figure 4.25. A PMBLDC machine is coupled with a flywheel is used to emulate the RB action. The steady-state capacitor voltage V_c, output voltage V_o, input current I_s and input voltage V_s in step-up or motoring mode operation are shown in Figure 4.36.

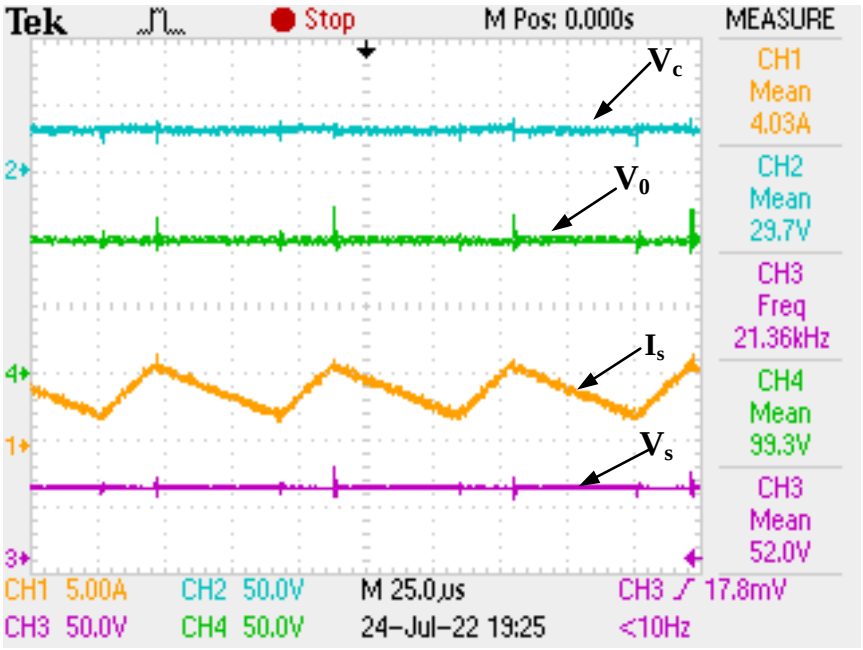

Figure 4.36: Capacitor voltage (V_c), output voltage (V_o), input current (I_s) and input voltage (V_s) during step-up operation.

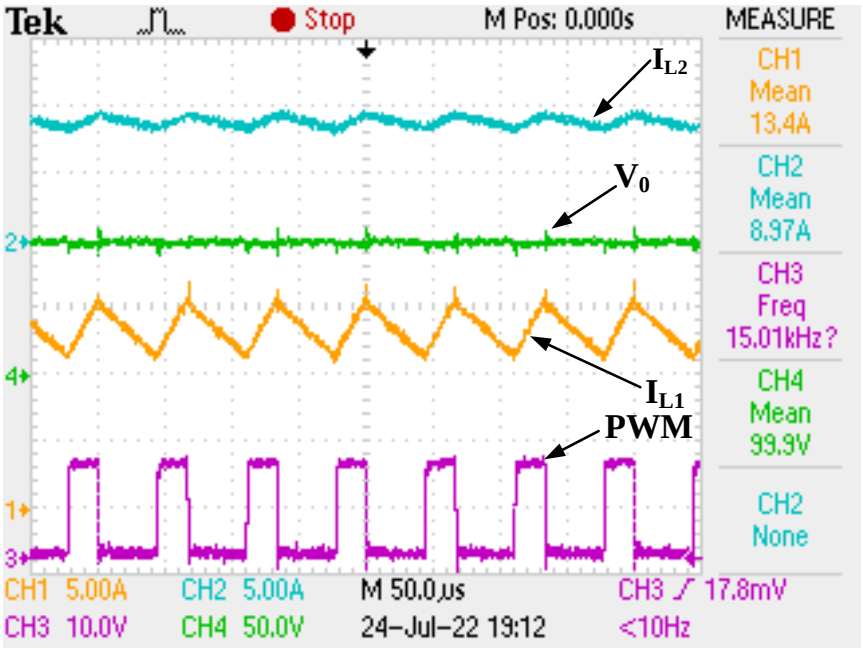

Figure 4.37: Inductors current (I_{L1}, I_{L2}), output voltage (V_o), and switching PWM during step-up operation.

The steady-state inductors current, output voltage with switching PWM during boost mode operation are illustrated in Figure 4.37.

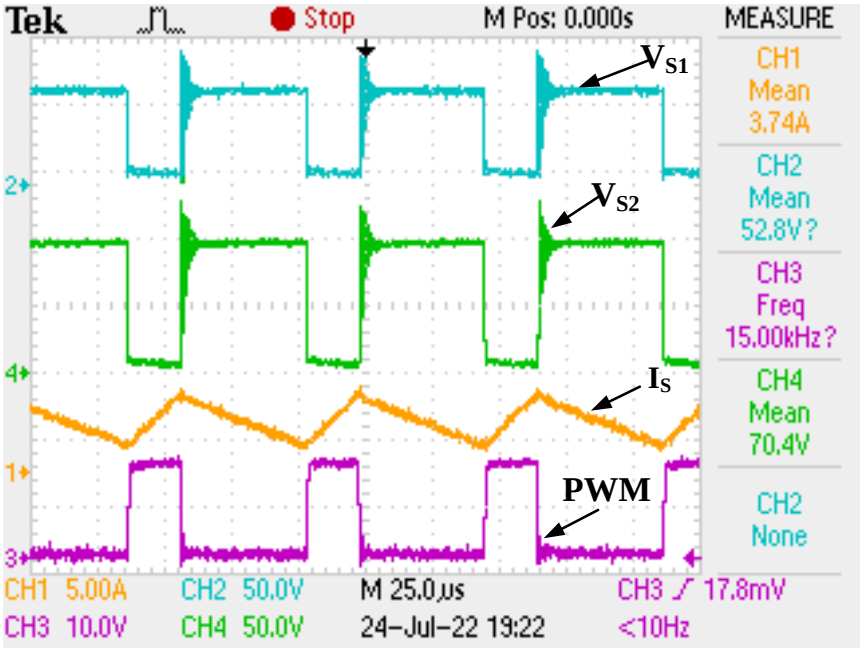

Figure 4.38: Voltage stress V_{s1}, V_{s2}, input current I_s with PWM during step-up operation.

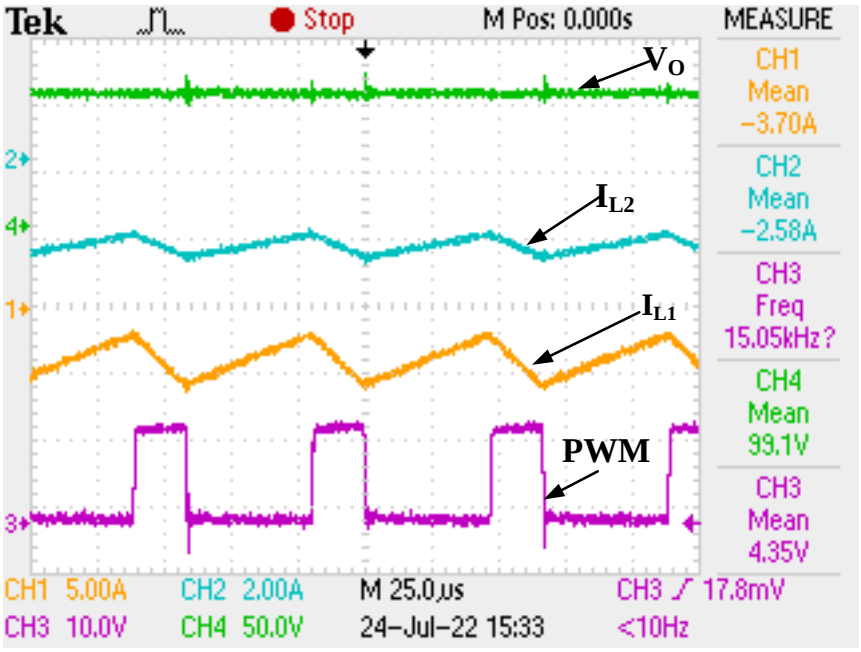

Figure 4.39: Inductors current (I_{L1}, I_{L2}), output voltage (V_o), and switching PWM during step-down operation.

The voltage stress on switches S_1, S_2, input current I_s with switching PWM are shown in Figure 4.38. The inductors current, output voltage with switching PWM during step-down or regenerative braking are shown in Figure 4.39. The three-switch control

strategy of VSI for RB of PMBLDC motor is done at different braking duty. The braking duty is varied from 0.4 to 0.7, the armature current, battery current, battery voltage, and command signal for RB action is illustrated in Figure 4.40. When the command signal is high, the PMBLDC motor acts in motoring operation and when the command signal goes low, the PMBLDC motor act as a generator in RB. One can see that as braking duty increases then the armature current, battery charging current, and braking torque increase.

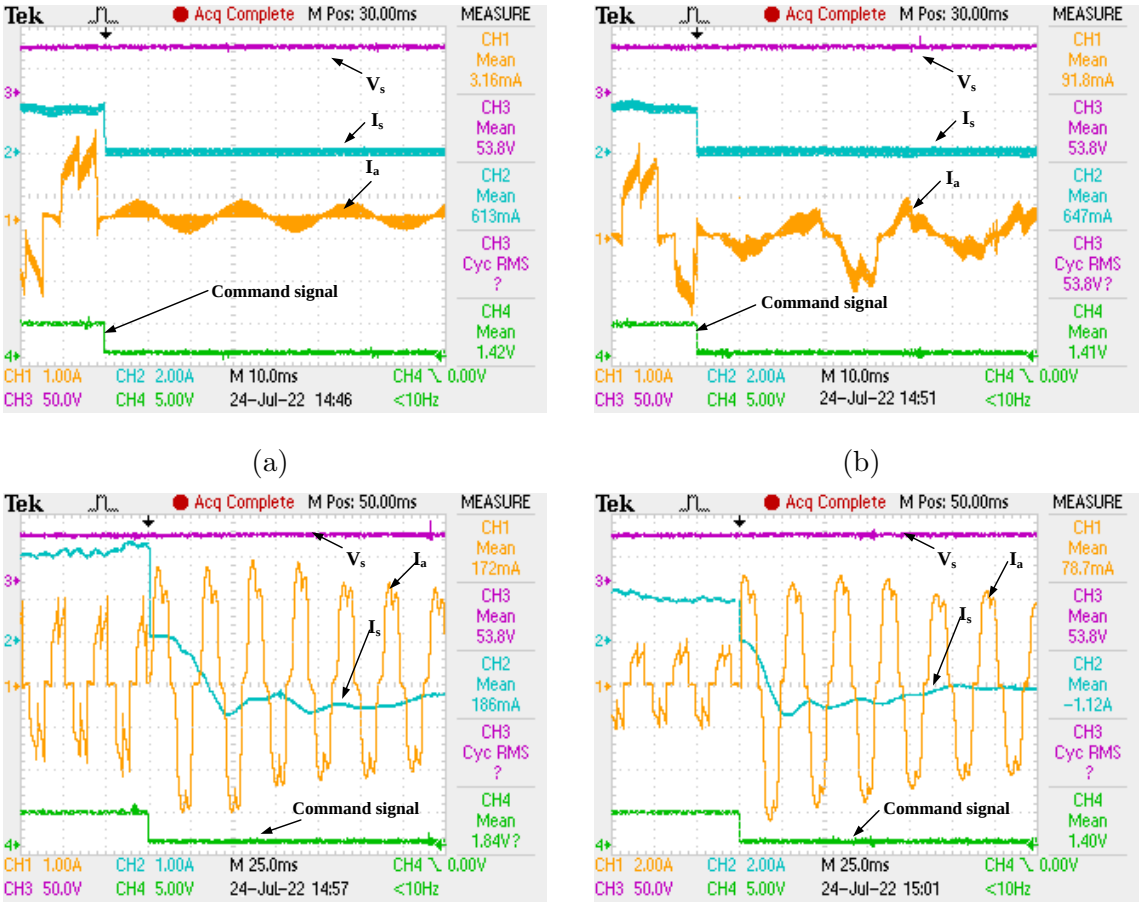

Figure 4.40: Armature current, battery current, battery voltage, command signal at different braking duty (a) $\delta = 0.4$ (b) $\delta = 0.5$ (c) $\delta = 0.6$ and (d) $\delta = 0.7$.

The efficiency of the proposed converter is calculated in MATLAB/Simulink while taking care of DC resistance of inductors, ON resistance of MOSFET, and diode forward voltage drop of MOSFET. The Figure 4.41 shows the % efficiency with respect to output power at constant output voltage. The output power is varied from 100 W to 1000 W during step-up operation of the converter.

The results obtained in experiment are compared with simulation results at two different output voltage and frequency for validation are done in Table 4.3 and 4.4.The speed of the motor during experiment is measured with stroboscope tachometer.

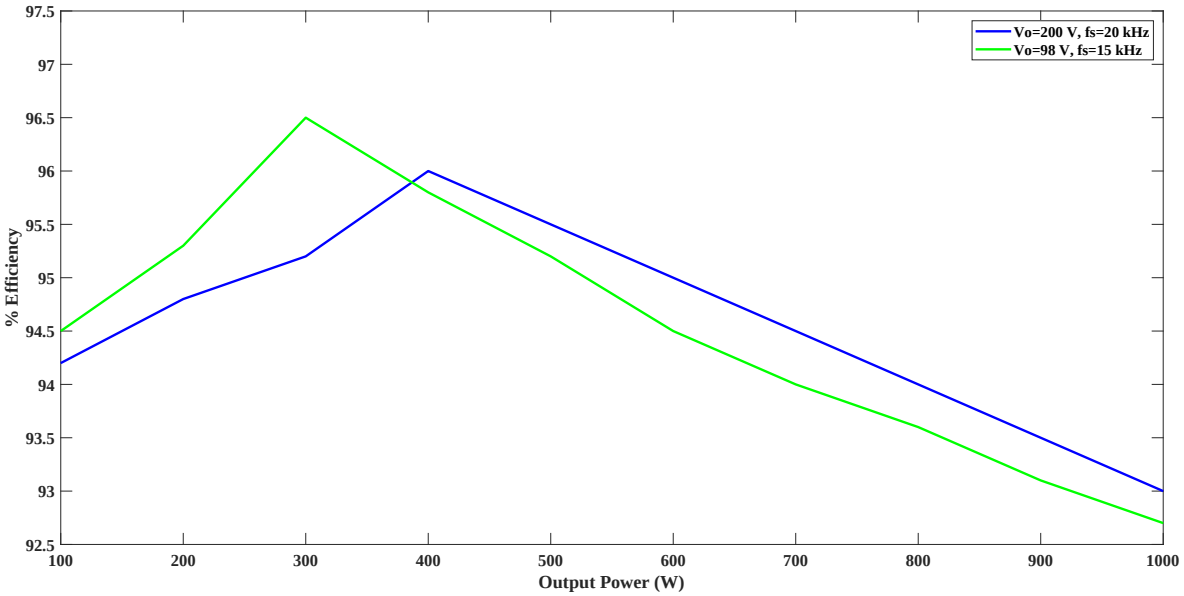

Figure 4.41: Converter efficiency during step-up operation with input voltage V_s=48 V.

Table 4.3: Comparison of simulation and experimental results for output voltage 200 V and operating frequency 20 kHz.

Parameters	Output Voltage V_o	Capacitor voltage V_{c1}	Input current I_s	Inductor current	Voltage stress	Motor speed
Simulation	200 V	102 V	9 A	I_{L1}=9 A I_{L2}=4.2 A	V_{s1}=V_{s3}=102 V V_{s2}=V_{s4}=200 V	3600 rpm
Experimental	202 V	104 V	9.2 A	I_{L1}=9.2 A I_{L2}=4.5 A	V_{s1}=100 V V_{s2}=202 V	3500 rpm

The comparison of different bidirectional DC DC converters with the proposed converter are done in Table 4.5.

Table 4.4: Comparison of simulation and experimental results for output voltage 98 V and operating frequency 15 kHz.

Parameters	Output Voltage V_o	Capacitor voltage V_{c1}	Input current I_s	Inductor current	Voltage stress	Motor speed
Simulation	98 V	28 V	13 A	I_{L1}=13 A I_{L2}=8.4 A	V_{s1}=V_{s3}=69 V V_{s2}=V_{s4}=98 V	1800 rpm
Experimental	99.9 V	29.7 V	13.4 A	I_{L1}=13.4 A I_{L2}=9 A	V_{s1}=V_{s3}=71 V V_{s2}=V_{s4}=100 V	1750 rpm

Table 4.5: Comparision of different bidirectional converters with proposed converter

Reference	Total components	Voltage ratio boost	Voltage ratio buck	Maximum voltage stress	Maximum Efficiency
Converter in [121]	1 coupled inductor 3 capacitors 4 power switches	$\frac{1}{(1-D)^2}$	D^2	$\frac{V_L}{(1-D)^2}$	90 %
Converter in [122]	4-winding coupled inductor 3 capacitors 4 power switches	$\frac{2(1+nD+kD)}{1-D}$	$\frac{(1-D)}{2(1+nD+kD)}$	$\frac{(1+n)V_H}{1+nD}$ & $\frac{V_H}{1+nD}$	93 %
Converter in [91]	3 inductor 6 capacitors 8 power switches	$\frac{3}{1-D}$	$\frac{D}{3}$	$\frac{1}{1-D}$	95.6 %
Proposed converter	2 inductors 2 capacitors 4 power switches	$\frac{1}{(1-D)^2}$	D^2	$\frac{1}{(1-D)^2}$	96 % (20 kHz) 96.5 % (15 kHz)

4.5 Conclusion

A modified QGBC is designed, developed, and tested for RB application in EV. The power flow direction is controlled successfully by changing the working mode of the VSI and the modified QGBC. In the regenerative braking mode, the inertial load's mechanical energy is changed to electrical energy and fed back to the battery, as evident from the results. A control strategy is implemented to boost the back EMF of the PMBLDC motor by controlling the VSI and using the self-inductance of the motor. The quadratic

gain bidirectional DC-DC converter operates at maximum efficiency of 96 % at an output voltage of 200 V and operating frequency 20 kHZ and 96.5 % at an output voltage 98 V and operating frequency 15 kHz during the converter's step-up operation. The implemented strategy and the system configuration present a frugal and practical approach to eliminate the drawbacks of regenerative braking in the buck mode of BDC.